WIRELESS ENGINEER

Vol. 32 NOVEMBER 1955 No. 11

Radio Communication by Wave Scattering

THE student of physics meets the problem of scattering when considering the re-radiation of light incident on minute particles of linear dimensions small compared with the wavelength. The intensity of this re-radiation from a single particle or vibrating unit was shown by Lord Rayleigh, some eighty years ago, to vary according to the relation $\sin^2\alpha/\lambda^4 d^2$, where α is the angle between the direction of vibration and that of the observer, λ is the wavelength and d the distance from the particle. When the light is incident on a collection of such particles, the intensity of the re-radiation in any direction depends upon the vectorial sum of the components received from all the particles regarded as secondary sources of radiation. The operation of the law involving the wavelength is demonstrated by the fact that the open sky appears blue when seen by scattered light; and that when the sun is viewed through light clouds or a haze of scattering particles, the light is red. Both these observations indicate that the short waves of blue light are scattered more effectively than the longer red waves, which therefore penetrate more than blue light through a scattering medium.

Scattering of Radio Waves

The phenomenon of the occurrence of scattering in the propagation of radio waves was first dealt with in a comprehensive manner in a remarkable series of papers published by T. L. Eckersley during the period 1927–1940. While at the beginning of this period there was still some uncertainty as to the number and position of the various layers in the ionosphere responsible for the reflection of waves, Eckersley deduced from his own theoretical research, supported by a vast amount of experimental data, that irregularities in one or other of these layers resulted in the scattering of waves incident upon them. It was appreciated that, for any given frequency, there was a minimum distance—termed the 'skip distance'—at which short waves could be returned to earth by reflection from a layer of a given density of ionization. Yet, it was shown, first that weak signals could on occasions be received within this skip distance, and secondly that, in the case of a beam transmitting station, these signals originated from the point at which the beam of radiation was incident on the ionosphere. Direction-finding observations showed that the latter point was the effective source of the received signals, and this was not necessarily in the same direction as that of the transmitting station. This experience is somewhat analogous to that of a searchlight directed on to clouds in the sky. Where the searchlight itself is hidden from the observer, the point of intersection of the beam of light and the scattering clouds appears to be the source.

In addition to this investigation of 'back-scattered' signals within the skip distance, Eckersley also carried out a comprehensive study of the scattering of signals experienced in long-distance communication. In this case it was appreciated that while the scattered signals were very weak compared with the normal strength of those arriving by regular reflection from the ionosphere, they were easily detectable both aurally and by photographic recording, especially during periods of fading of the normal signals due to the occurrence of conditions of wave interference or high absorption. The records of Eckersley and of other workers in Europe and America showed that scattering of radio waves could occur on all wavelengths from 15 to 210

metres, but the general experience indicated that the phenomenon was more prevalent with the shorter waves.

What does not appear to have been appreciated in the 1930–40 decade is that if the wavelength were reduced below that corresponding to the critical or maximum-usable frequency for a given path, then there would be no signals received by regular reflection, but there might still be useful radiation arriving by the scattering process from the irregular or 'sporadic' regions of intense ionization in the ionosphere.

In the course of research on the characteristics of the ionosphere during the past quarter of a century, a great deal has been learnt about the phenomena associated with the scattering of radio waves from irregularities in the ionosphere. In the E region in particular, several types of scattering sources have become recognized and described more-or-less definitely under such titles as sporadic-E, meteoric-E and auroral-E. But the reception of signals resulting from radio-wave propagation in which these regions play a part has always been regarded as very intermittent and unreliable, and subject to large diurnal and seasonal variations. The majority of the observational work has therefore been largely confined to the determination of the extent, thickness and height of these regions regarded as irregularities in the ionosphere, and to studying their horizontal movement over various distances, rather than to considering how the irregularities might be made use of in practical radio communication.

Scattering in the Troposphere

The interest which has arisen in recent years in the communication aspects of wave propagation by forward scattering in the ionosphere appears to have been stimulated, curiously enough, by a theoretical and experimental study of the corresponding conditions for the scattering of radio waves in the troposphere. In a paper published in 1950, H. G. Booker and W. E. Gordon reviewed previous experience on the propagation of centimetre waves in the lower atmosphere in the light of the relevant meteorological knowledge of conditions of turbulence in the atmosphere. It was realized that such turbulent motion could result in the formation of volumes of air of linear dimensions of the same order as or larger than the wavelength, in which the refractive index fluctuated in relation to that of the surrounding air, and so could produce significant scattering of short radio waves. With these ideas in mind, the theory of scattering in a medium with randomly-distributed inhomogeneities which had been previously developed in connection with the propagation of sound in water, was reformulated for radio-wave transmission conditions. In the analytical treatment, formulae were derived for the intensity of the scattered radiation in both forward and backward directions from the transmitter, in terms of the departures of the refractive index from the average value and the 'scale of turbulence', or the dimensions of the irregularity in relation to the wavelength. It was shown as a typical case, that for large values of $2\pi l/\lambda$, where l is the scale of turbulence, the scattering is mainly confined to the forward direction and within an angle equal to the reciprocal of this quantity.

In seeking for experimental confirmation of this analysis, it was appreciated that at reasonably short ranges from a transmitter, the contribution of field strength from scattering would be chiefly evident as fading due to interference with the field arriving at the receiver by conventional propagation. While, however, the energy represented by the latter field decreases inversely as the square of the distance, the scattered energy is inversely proportional to the distance. It might reasonably be expected therefore that at some distance the fields due to the two different modes of propagation would become equal and that from there onwards, the rate of attenuation with distance would be greatly reduced. Booker and Gordon show that this reasoning was very well confirmed by experimental results reported by Katzin for transmissions in the Caribbean Sea on a wavelength of 9 cm. For short distances the rate of attenuation of field strength followed the conventional mode theory; but at about 80 miles from the transmitter there was a sudden decrease in this rate, and from this point out to 160 miles, there was a much less rapid decrease in field strength. These results are consistent with what would be expected for scattering in a medium with a scale of turbulence somewhat larger than the wavelength in use. An independent analysis of this problem has also been published by E. C. S. Megaw, who, in addition, has given supporting evidence from experiments conducted in the North Sea on a wavelength of 10 cm up to distances of 300 miles. While little practical information has so far been published, there have been definite indications that the possibilities of exploiting this technique of forward scattering in the troposphere for frequencies above 300 Mc/s and up to distances of the order of 300 miles (500 km), are quite favourable.

Propagation by Ionospheric Scattering

As already mentioned, it was probably due to the stimulation provided by the work described above that led a group of scientists associated with the United States National Bureau of Standards to investigate the possibilities of detecting

scattered radiation arising from turbulence in the ionosphere when other forms of ionospheric transmission are absent. A paper published in 1952 under the names of eight authors (D. K. Bailey et al.) contains a description of experiments conducted between a transmitter at Cedar Rapids, Iowa, and a receiver at the Sterling, Virginia, station of the Bureau of Standards. The power supplied to the transmitting aerial was about 23 kilowatts, at a frequency of 49·8 Mc/s, and the length of the above path was 1,245 km (780 miles). Using a receiver bandwidth of 3 kc/s, the experiment was immediately successful under the above conditions. Owing to the rapidly varying nature of the signal, the received power was recorded automatically, using an averaging circuit having a time constant of 12 seconds. The received field-strength was of the general nature of a reasonably steady background signal due to the scattering process, on which were superposed from time to time other signals of much greater strength, considered to arise from the incidence of sporadic-E or meteoric-E conditions in the ionosphere. The scattered signal, which was always present, showed a diurnal variation of some 12 dB in April and 16 dB in June 1951, with a maximum at about noon and a minimum at about 2000 hr local time in each case. April observations showed a less prominent secondary maximum at about 0600; and this suggested to the authors that the received signal resulted from two basic causes. One of these is solar ultraviolet radiation which produced the noon maximum; and ionization due to meteors is known to produce a maximum at about 0600 and a minimum at 1800 hr. Another feature of the experimental results, and one which is of great importance in connection with practical communication, is that the received background signal due to scattering appears not to be seriously affected by magnetic storms or ionospheric disturbances. Indeed, the occurrence of such disturbances was found to cause an increase of some 3 to 9 dB in the received signal on occasions.

Although there is little further published literature available, the continuation of the above investigations in U.S.A. was described by D. K. Bailey at the General Assembly of the International Scientific Radio Union (U.R.S.I.) at The Hague in August 1954, and later at the meeting on "The Physics of the Ionosphere" at the Cavendish Laboratory, Cambridge. Experiments were made to determine the height at which scattering takes place by two methods, one using pulse modulation at the transmitter, and the other making use of a knowledge of the vertical polar radiation diagram of the transmitting aerial. Both methods led to the conclusion that the scattering occurred at a height of about 75–80 km by day and 85–90 km by night. Next the dependence of the received power on the frequency used was investigated. Using aerial systems scaled in proportion to the wavelength, and adjusting the results to correspond to equal receiving apertures, it was found that comparing frequencies of 50 and 108 Mc/s the received power was inversely proportional to f^8, whereas a corresponding experiment comparing 50 and 28 Mc/s gave a value of f^6.

The theories of scattering discussed above indicate that the received power should vary with the frequency (f) inversely proportional to f^n, where $n = 8$ according to Eckersley's theory published in 1932, and $n = 4$ on Booker and Gordon's theory. It is clear that further experimental confirmation is required before a firm relationship of variation of propagation conditions can be established.

Further results of the extended observations are that the scattered radiation was found to fade with a quasi-frequency of a few cycles per second, and that the received wave-front showed greater coherence in the direction of propagation than across it. In agreement with this last result, it was found that the large directive aerials used did not provide the gain calculated for coherent plane waves, the actual realized gain being greater when the received signals were strong.

Experiments in the United Kingdom

At a meeting of the Radio Section of the Institution of Electrical Engineers on 31st October a paper was presented by W. J. Bray, J. A. Saxton, R. W. White and G. W. Luscombe describing an investigation, which had been in progress since 1952, of the propagation of v.h.f. radio waves by scattering from the E-region of the ionosphere. The transmitting station was installed in the Shetland Islands, and recording of the received signals was carried out at a Post Office station in Jersey over a distance of 1,185 km (740 miles), and at the D.S.I.R. Radio Research Station, Slough, at 935 km (580 miles). Additional observations were conducted by the Admiralty in a ship which traversed an arc of some 30° away from the maximum of the beam of radiation from the transmitter: this beam was some 7° wide in elevation and 10° in azimuth (to 3 dB below the maximum). The results of these experiments have largely confirmed the experience in America as to the relatively steady nature of the background signal, which was found to be suitable for telegraph transmission or for commercial telephony in a bandwidth of not more than 3 kc/s over distances up to about 1,200 miles; though

somewhat different detailed conclusions have been reached concerning the dependence of the scattered energy on frequency. The British work does, however, indicate a rapid decrease in scattered energy with increasing frequency, and shows that the range of frequencies for which ionospheric scattering is likely to afford a useful means of communication is about 25 to 60 Mc/s. The fact that radio circuits operating on this basis are relatively immune from ionospheric storms offers possibilities for their use in commercial practice in spite of the relatively high transmitting power and narrow bandwidths that must be employed. R.L.S-R.

DETECTION OF PULSE SIGNALS IN NOISE

Theory of Intensity-Modulated Display in Terms of Just-Noticeable Differences

By D. G. Tucker, D.Sc. and J. W. R. Griffiths, B.Sc.

(Department of Electrical Engineering, University of Birmingham)

SUMMARY.—A Just-Noticeable Difference (j.n.d.) is defined as the increment of applied voltage (or current) which can cause with certainty a just-noticeable increase in intensity on an intensity-modulated visual display. The size and number of j.n.ds form a subjective measure of the display characteristics, being determined by averaging results obtained by a number of observers. This paper presents a theory of detection of pulse signals against a noise background in terms of j.n.ds, with some simple numerical illustrations. It is shown that while the basic conceptions of the measurement and use of j.n.ds are sound, and are fundamentally related to the performance of displays as detecting devices, yet in practice there are many complicating factors that are difficult to take into account. It is thus not clear how accurately it will be possible to predict display performance. However, there is no doubt that the total number of j.n.ds which can be measured between the marking threshold and the saturation level of the display medium (this number determining the smallness of each individual just-noticeable increment) is a measure (albeit far from linear) of the efficiency of the display. It is also likely that extension of the theory developed here could lead to an overall optimizing of the design of receiver circuits and displays on a basis of non-linear response; the object would be to use the most sensitive detection at voltage levels where the probability of detection is greatest.

LIST OF SYMBOLS

Probabilities

$p_N(A)$ = probability distribution of noise amplitudes

$p_S(A)$ = probability distribution of signal-plus-noise amplitudes for a given signal/noise ratio

J.N.Ds

R = number of just-noticeable increments from zero to saturation amplitude

δ = size of j.n.d.

Amplitudes

A = amplitude in general

A_m = amplitude at which the display just commences to mark or paint; i.e., the marking threshold

A_{sat} = amplitude at which saturation occurs

Also

T = duration of scan in secs

B = bandwidth of receiver in c/s

n = TB

$^mC_b = \dfrac{m!}{b!\,(m-b)!}$

1. Introduction

AMONG the problems associated with the visual detection of pulse signals against a noise background on an intensity-modulated display there is one which has received much less attention than the others; it is the problem of how to relate measurable objective and subjective characteristics of the display medium to the detection threshold of the signal. To state the problem more formally, how can the probability of detection of the signal at any given signal/noise ratio be related to the measurable qualities of the cathode-ray tube and its phosphor or of the chemical recorder[2] and its iodized paper?

There are several measurable qualities which influence detection, and among the most important are:—

(a) Spot size in cathode-ray displays and stylus size in chemical recorders.

(b) Duration of afterglow in cathode-ray tubes and factors such as degree of overwriting and speed of paper in chemical recorders.

(c) Texture or uniformity of mark made by a constant d.c. applied to display—in other words, 'graininess' or 'false noise'.

(d) Magnitude of the change in applied voltage or current required to produce with certainty a just-noticeable difference (j.n.d.) in the marking.

MS accepted by the Editor, February 1955

(e) Number of such changes in the dynamic range of the display; i.e., how many increments which just cause an observable change in marking can be made successively between zero-marking and saturation?

These are not all independent effects, as some interact with others.

The purpose of the present paper is to show some of the ways in which the size and number of j.n.ds affect the detection of pulse signals against a noise background, and a simple theory of detection in terms of j.n.ds is developed. A simple numerical example illustrates the type of result which is obtained from this theory, and it is clear that some empirically-known features of visual detection can be explained in terms of it. The difficulties of extending the theory are briefly reviewed.

2. Definition and Measurement of J.N.Ds

Before discussing the theory, it is necessary to define a just-noticeable difference and show how it can be measured.

Being measured by human judgment, j.n.ds are subjective quantities. It is necessary to take measurements with several different persons, therefore, in order to obtain reliable average values. The quantity actually measured on any one occasion is the increment of voltage or current required to cause a new mark on the display to be judged as just-noticeably brighter (or darker, as the case may be) than the previous mark. This measurement is made at all marking intensities from the marking threshold up to saturation, and a continuous function can be plotted relating size of j.n.d. (expressed as a ratio or as an arithmetic increase) to voltage, current, or intensity level. If the measurement is made so that each successive increment follows from the one below it, then the total number of increments that are made between marking-threshold and saturation is the number of j.n.ds in the dynamic range of the display medium.

The theory developed in this paper is built round a j.n.d. which is certain; i.e., the test is so conducted that it is nearly 100% certain that the increment which the observer thought was just noticeable was in fact truly noticeable. This is readily ensured by making the initial mark across the whole display, but the increased mark in one particular position within the initial mark; the position must be correctly identified on several successive repetitions at the same initial level with the increased mark located at random. The test can thus be designed to any desired degree of certainty. Measurements with which the authors have been associated have been designed to achieve 97% certainty.

In general, j.n.ds are not uniform either in ratio or voltage or current, but are smaller in the central part of the dynamic range than at the extremes. A typical average curve of size of j.n.d. (expressed as a ratio $\Delta V/V$) against position in the voltage range is shown in Fig. 1 for a cathode-ray tube type CV429 used under standard conditions in a very dark room. The average total number of j.n.ds obtained by several observers was about 40. This number is probably reduced considerably when some ambient illumination is used in the room.

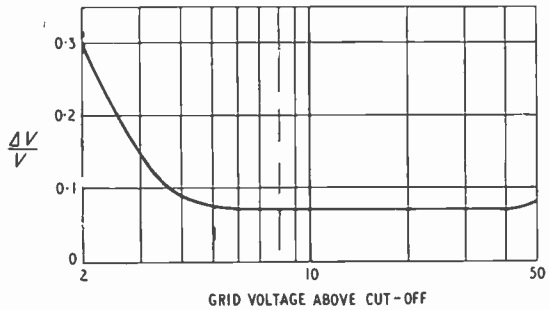

Fig. 1. *Typical curve of size of j.n.d. against voltage level for cathode-ray tube.*

3. Simple Theory of Detection in Terms of J.N.Ds

In this section we shall attempt, by simplifying the conditions and ignoring certain difficulties, to show the relationship between detection and j.n.ds in general terms. In this way the fundamental points can be brought out. The simplifications and difficulties will be discussed later. A mathematical analysis of the theory is set out in Appendix 1.

Consider a display giving an intensity-modulated visual presentation of a single 'scan' or, in more exact terms, presenting a single pulse against a background of noise in such a way that intensity of paint or marking represents the amplitude of the applied waveform, and position across the display represents time. The pulse can be detected against the noise background only by virtue of

(a) Having a larger amplitude than the largest peak of noise present on the scan, or

(b) Having an envelope shape different from that of the noise peaks.

If the optimum bandwidth is used, the envelope shape of the pulse is the same as that of the noise peaks, and then (b) does not arise. Consider such a case where an ideal display is used, i.e., one where the size of j.n.d. is infinitely small. Then the probability of detection is the probability that the signal pulse causes a peak amplitude of signal-plus-noise (a 'signal peak') larger than the largest peak of noise alone. This probability

can be readily calculated. [Equation (3) of Appendix 1.]

Now suppose the j.n.d. has a finite size but that there is still an infinite range of dynamic response. Then a 'signal peak', to be detected with certainty at any level, must exceed the largest noise peak by one j.n.d., or it can be detected with 50% probability if one noise peak comes within one j.n.d. above or below it, or with 33% probability if two noise peaks come within this range, and so on. The overall probability of detection is the integrated effect of this detection over the whole range of applied signal-plus-noise level. This can also be calculated, as set out in Equation (9) of Appendix 1.2. The reduction in the probability of detection can thus be related to the size of a j.n.d.

The assumption of an infinite range of dynamic response was, of course, very unrealistic. It is clear that when there is only a finite number of j.n.ds in the range of response of the display (i.e., between minimum marking and saturation) there is a possibility that a large noise peak will leave less than one j.n.d. available above it, so that no larger peak can be distinguished from it on a basis of amplitude. Thus on the particular scan in which this large noise peak occurs, the probability of detection of a signal is reduced because even if it does reach or exceed this noise level, it is only a 0·5 probability that the correct peak would be chosen. Similarly if there are two noise peaks of this high level, it is only a 0·33 probability of a correct choice, and so on. The full analysis is given in Appendix 1. The effect of marking threshold and contrast by bias is also taken into account in Appendix 1.

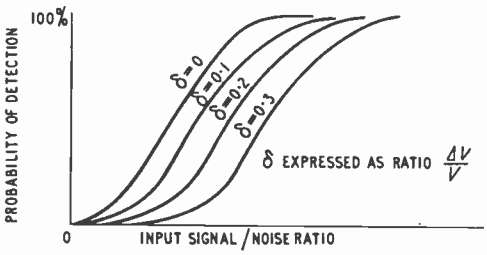

Fig. 2. *Probable type of relationship between detection and signal/noise ratio for various values of δ (size of j.n.d.) and for fixed values of marking and saturation levels and r.m.s. noise input.*

The above discussion shows the basic effects of size and number of j.n.ds. Further factors which complicate the determination of thresholds still more are discussed in a later section. For now we may reasonably conclude that both size and number of j.n.ds are important; a large size and small number leads to a reduced probability of detection. Of course, if the marking and saturation levels are fixed, then the number of j.n.ds is in any case determined by the size and vice versa.

Although Appendix 1 sets out the mathematical statement of the probabilities of detection in terms of j.n.ds, it is to be noted that numerical calculations from the formulae given are not easy, since when actual probability distributions are substituted for $p_S(A)$ and $p_N(A)$ the integrations are not straightforward, and numerical integration would be very laborious. Consequently no numerical results have yet been worked out for actual practical cases. In their absence, Fig. 2 shows the *type* of numerical relationships that might be expected between detection probabilities, j.n.ds and input signal/noise ratio. A separate set of graphs would be needed for each set of values of marking and saturation levels expressed as ratios of the r.m.s. noise input, and for each value of the product (time of scan) × (bandwidth).

In spite of this difficulty of calculation, a considerable insight into the significance of j.n.ds and other display limitations can be obtained by calculating a grossly-simplified case in which the difficulties are minimized. This is done in the next section.

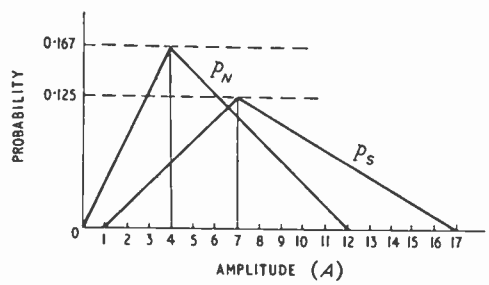

Fig. 3. *Probability distributions used in numerical example. The amplitude scale is in arbitrary units of voltage or current.*

4. Simple Numerical Example

This very simple case is one in which the probability distributions $p_N(A)$ and $p_S(A)$ have been each reduced to two straight lines, giving triangular graphs as shown in Fig. 3. The distribution of noise peak amplitudes, $p_N(A)$, is made to resemble the Rayleigh distribution, and the distribution of 'signal peaks', $p_S(A)$, is made to correspond very approximately to a signal/noise ratio of +2 dB. The area under both graphs is, of course, unity. A comparison of the parameters of these distributions with the true distributions is given in Appendix 4. It can there be seen that the resemblance is very good.

The calculations have been made along the lines of Appendix 1, and the results are summarized in Table 1. It is assumed that the product, (time of scan) × (bandwidth) is equal to 21. As

it is very instructive to follow through the calculations to some extent, the initial stages of the work are set out in Table 2.

For simplicity, j.n.ds have been taken as of equal size in terms of voltage or current units, not as ratios. This is more favourable to detection, and worse detection for a given number of j.n.ds would have resulted from taking equal ratios. As it is, it can be seen that the probability of detection is reduced when the j.n.ds are increased in size from 0 to 2, and their number reduced to 9 over the range of applied voltage or current. It is clear from the calculations that the probabilities of detection are negligible over the voltage or current range from 0 up to about 7, although this is almost half-way along the total range. This means that it is very inefficient to retain this lower range of response, and when there is only a limited number of j.n.ds available, it is better to use contrast on the display and distribute the available j.n.ds where they are more effective. On the other hand, severe loss of detection results when saturation by noise peaks is permitted. Thus we see, from Table 1, that if only about 10 j.n.ds are available, best results (29% probability of detection) are obtained when the marking threshold is set at 7 units and saturation is just avoided, intermediate results (24·5%) when the whole range is accommodated without contrast or saturation, and rather poorer results (16%) when no contrast is used and saturation occurs at 10 units.

It is thought that these results are of much wider application than the simplified calculations might at first sight suggest, and they are in accord with experience.

TABLE 1
Results of Numerical Example

Size of j.n.d. (arithmetic increment)	Number of j.n.ds	Saturation Level	Marking Level	Probability of Detection (%)
0	∞	17 or over	0	30·4
1	17 or more	17 or over	0	28·9
2	9 or more	17 or over	0	24·5
0	∞	10	0	24·0
1	10	10	0	16·1
1	10	17	7	28·9

The figures in Columns 1, 3 and 4 are in units of voltage or current.

N.B.—For this example, $TB = 21$, where T = time of scan, B = bandwidth of receiver.

TABLE 2
Some Stages in the Computation of the Numerical Example

A	$\int_0^A p_N(\cdot A).dA$	$\left[\int_0^A p_N(\cdot A).dA\right]^{20}$	$p_s(A)$	$p_s(\cdot A)\left[\int_0^A p_N(\cdot A).dA\right]^{20}$
1	2/96	—	0	
2	8/96	$<10^{-21}$	1/48	
3	18/96	$<10^{-14}$	2/48	Negligible
4	32/96	$<10^{-9}$	3/48	
5	47/96	$<10^{-6}$	4/48	
6	60/96	0·000083	5/48	
7	71/96	0·0024	6/48	0·0003
8	80/96	0·0263	9/80	0·0030
9	87/96	0·1445	8/80	0·0145
10	92/96	0·4365	7/80	0·0390
11	95/96	0·7945	6/80	0·0600
12	1	1	5/80	0·0625
13	1	1	4/80	0·0500
14	1	1	3/80	0·0375
15	1	1	2/80	0·0250
16	1	1	1/80	0·0125
17	1	1	0	0

5. Simulation of J.N.D. Behaviour by Use of a Display Consisting of Discrete Amplitude-Gates

A consideration which would have a bearing on a practical study of the effects of j.n.ds in visual displays is whether or not the performance of the display system can be simulated by an artificial system in which gating circuits, operating at pre-set levels and responsive only to the peaks, represent the operation of j.n.ds. The gates would indicate the interval of amplitude into which each successive peak falls, so that the scan would be presented as a series of numbers (in effect), of which the highest is presumed to be the signal. Such a system could be made without undue difficulty, and the effect of size and number of intervals and their non-uniformity could then be studied with much less trouble than the corresponding effects with real displays. But j.n.ds do not operate between fixed voltage levels—a j.n.d. is an increment from *any* particular level which happens to be relevant, and in the integrations of Appendix 1, *all* levels are considered in a continuous manner.

Appendix 2 shows how the probability of detection in the gated system can be calculated. If this method is applied directly to the signal and noise peak-amplitude distributions of the previous numerical example (Fig. 3), and the gates are set to operate at intervals of two voltage or current units, then the probability of detection works out at 0·29; i.e., the same as for a real visual display with j.n.ds of one unit.

In general, it would seem that gated intervals of two j.n.ds should give a good representation of visual display performance.

It should be noted that all the above calculations depend on detection being on a basis of choosing the largest-amplitude peak, and ignore all considerations of detecting by other factors, such as pulse length when it is not the reciprocal of the bandwidth.

6. Further Considerations

In practice, the following further factors are among those which have to be considered in calculating the influence of j.n.ds on detection.

The previous discussion considered only single scans—but in practice successive scans are usually allowed, or made, to add together in some way; e.g., afterglow in cathode-ray displays produces very effective adding at high repetition rates, and the scan-to-scan correlation or addition in chemical recorders has a similar effect which is not yet fully explored[3]. If the addition is linear, the calculation of the probabilities of detection should be little more difficult than for the single scan*.

By the use of bias, or square-law detectors, etc., it is possible to modify the effective input signal range, and so alter the detection thresholds. Provided that any sort of non-linear law can be arranged, it is clear that the detector-plus-display system can be optimized by 'matching' the non-linear distortion to the characteristics of the display. For example, the marking threshold and saturation levels can be freely chosen, the size of the j.n.ds of the overall system can be made unequal if desired and suited to the different probabilities of detection at the various levels of input amplitude, and so on. Theoretically and practically, this process is likely to be very difficult, but may be very important. Once the principle is accepted, however, it can be seen that the size of j.n.d., although a factor in calculation, is no longer an inherent parameter of the system, and the number of j.n.ds available is the only fixed, fundamental, quantity. A first approach to this optimizing process was illustrated in Section 4.

Another serious difficulty is that the size of a j.n.d. is probably a function of how far separated along the time scale are the 'signal peak' and the largest noise peak. The measurements of j.n.ds are normally made with the various levels adjacent to that against which comparison has to be made. When there is a considerable spatial separation of the levels being compared, the just-noticeable difference is almost certainly larger. Thus calculations of probability of detection would have to include the probability distribution $p(S)$ of the spacing S between the 'signal peak' and the largest noise peak, and would have to allow for the size of the j.n.d. δ being a function $\delta(S)$ of the spacing. A similar complication arises from the fact that even without this spatial effect, there is really a probability distribution associated with the size of j.n.ds owing to the figures used in the calculations being only an average of subjective observations.

The effect of shape of the signal pulse envelope relative to that of the noise—i.e., the influence of the product (bandwidth) $\times$ (pulse-length)—is not easily calculated*.

All the above work has considered the display as consisting of a single-line intensity-modulated presentation. Further extensions of the theory will be necessary to cope with p.p.i. and B-scan displays*.

It is clear that a comprehensive theoretical assessment of display performance in terms of j.n.ds is likely to be an extremely difficult and complicated undertaking. The only consolation is that assessment in any other terms is not likely to be any easier!

7. Conclusions

The results of this preliminary and non-rigorous study of the performance of displays in terms of j.n.ds show that the method is basically sound and that j.n.ds (number and/or size) can be used as a basis for the comparison and assessment of the merits of various display media and of whole detector-plus-display systems. But for the use of j.n.ds to be anything other than a crude first approximation, some difficult conceptions and measurements—additional to those involved in the simple mathematical analysis presented here—will have to be worked out. It will thus be some time before display performance can be accurately predicted. In the meantime, however, the preliminary calculations illustrated in this paper can certainly assist materially in practical design work.

It is to be noted that no other method of treating display problems has yet been published which shows any greater promise—so far as the authors are aware—and it therefore appears well worth while to follow up the present work. One particular direction in which improvement in performance (as distinct from the assessment of performance) may be found is the non-linear processing of the input signal to 'match' it to the display characteristics.

* McGregor (3) gives a brief discussion with numerical results of these three factors in relation to detection on various kinds of display; and on his basis it is suggested that an approximate method of extending the present work, from single scans with pulse duration equal to the reciprocal of the bandwidth, to multiple scans with longer pulses, is to increase the input signal/noise ratio used for calculation by about 2·2 dB for each doubling of the number of scans written side-by-side which contain the signal and for each doubling of the pulse length. For superposition of traces, the increase should be 1·5 dB per doubling. These figures assume that the initial input signal/noise ratio is below unity.

Acknowledgment

This paper was prepared while the authors were at H.M. Underwater Detection Establishment, and is published by permission of the Admiralty.

REFERENCES

[1] S. O. Rice, "Mathematical Analysis of Random Noise", *Bell Syst. Tech. J.*, January 1945, Vol. 24, p. 102.

[2] D. G. Tucker and J. W. R. Griffiths, "Detection of Pulse Signals in Noise", *Wireless Engineer*, November 1953, Vol. 30, p. 264.

[3] P. McGregor, "A Note on Trace-to-Trace Correlation in Visual Displays: Elementary Pattern Recognition", *J.Brit.I.R.E.*, June 1955, Vol. 15, p. 329.

APPENDICES

1. Theory of Detection and Just-Noticeable Differences

1.1. *Simple Ideal Case*

When 'white' noise has been restricted to a bandwidth B c/s, independent samples of information can be obtained only at times greater than $1/B$ sec apart; i.e., the number of independent pieces of information in a time T is BT. Since the number of peaks of the noise waveform is also approximately BT*, and they are spaced approximately $1/B$ sec apart, it is sufficient for most purposes to regard the peak amplitudes as the independent samples of information which define the noise characteristics. The function $p_N(A)$ governing the probability of a noise peak having any particular amplitude A will be of the form shown in Fig. 4. A similar distribution, but displaced to the right, will apply for the peak amplitude of the combination of signal and noise, say $p_S(A)$.

Now if we display one pulse of signal on a single scan of an intensity-modulated display with a time base of length T then the probability of detection can be calculated as below. The duration of the signal pulse is taken as $1/B$ sec, so that detection can be made on a basis of amplitude alone; there is no question of difference of shape or pattern.

If we assume that one of the peaks is due to a combination of signal-plus-noise then the probability of its having a particular amplitude A is $p_S(A)$.

The probability that the noise will not exceed A on any of the other peaks is

$$\left\{\int_0^A p_N(A)\,dA\right\}^{n-1} \qquad (1)$$

where $n = BT$.

Therefore the probability that, when the 'signal peak' has an amplitude A, it will be greater than any other peak is

$$p_S(A)\left\{\int_0^A p_N(A)\,dA\right\}^{n-1} \qquad (2)$$

Hence, if the j.n.ds of the display are infinitely small, the overall probability of detection is given by

$$\mathbf{P}_D = \int_0^\infty p_S(A)\left\{\int_0^A p_N(A)\,dA\right\}^{n-1} dA \qquad (3)$$

Strictly speaking, this is the probability of detecting the signal in one particular position out of n possible positions in the scan; the *a priori* probability of the signal being in that particular position is $1/n$, but since the overall probability is n times that for one position, this consideration does not affect the result in this case.

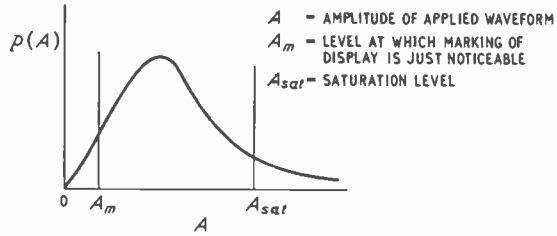

Fig. 4. *Type of probability distribution concerned.*

1.2. *J.N.Ds of Finite Size*

Suppose next that the j.n.ds are finite such that a difference of amplitude δ† is required to distinguish two peaks.

Now, therefore, detection will be made when

(a) at any 'signal peak' level of A the noise peaks do not exceed a level of $A - \delta$.

(b) at any 'signal peak' level of A the noise produces a peak (or several peaks) in the region $A \pm \delta$. If one of the noise peaks lies in the range $A \pm \delta$, since it is indistinguishable from the signal, we have only one chance in two of selecting the correct peak. Similarly if there are two noise peaks we have only one chance in three.

In case (a), probability

$$\mathbf{P}_1 = \int_0^\infty p_S(A)\left[\int_0^{A-\delta} p_N(A)\,dA\right]^{n-1} dA \qquad (4)$$

In case (b), the probability of any one noise peak lying in the range $A \pm \delta$ with the others below $A - \delta$

$$= \left[\int_{A-\delta}^{A+\delta} p_N(A)\,dA\right]\left[\int_0^{A-\delta} p_N(A)\,dA\right]^{n-2} \qquad (5)$$

Since it does not matter which noise peak is in this range we must multiply this probability by the number of noise peaks; i.e., $n - 1$.

Therefore the probability of detection for this condition

$$= \frac{n-1}{2}\int_0^\infty p_S(A)\left[\int_{A-\delta}^{A+\delta} p_N(A)\,dA\right]\left[\int_0^{A-\delta} p_N(A)\,dA\right]^{n-2} dA \qquad (6)$$

A similar argument applies to the remaining cases, so that if we put $m = n + 1$, the total probability is given by

$$\int_0^\infty p_S(A)\left\{\left[\int_0^{A-\delta} p_N(A)\,dA\right]^m + \frac{m}{2}\left[\int_{A-\delta}^{A+\delta} p_N(A)\,dA\right]\left[\int_0^{A-\delta} p_N(A)\,dA\right]^{m-1} + \ldots \right.$$
$$\left. \frac{m(m-1)(m-2)\ldots(m-b+1)}{1.2.3.\ldots b(b+1)}\left[\int_{A-\delta}^{A+\delta} p_N(A)\,dA\right]^b\left[\int_0^{A-\delta} p_N(A)\,dA\right]^{m-b} + \ldots\ldots\right\} dA \qquad (7)$$

$$= \int_0^\infty p_S(A)\sum_{b=0}^{b=m}\frac{1}{b+1}\,{}^mC_b\left[\int_{A-\delta}^{A+\delta} p_N(A)\,dA\right]^b\left[\int_0^{A-\delta} p_N(A)\,dA\right]^{m-b} dA \qquad (8)$$

Using the expression derived in Appendix 3 this can be shown to be

$$\mathbf{P}_D = \int_0^\infty p_S(A)\,\frac{\left\{\int_0^{A+\delta} p_N(A)\,dA\right\}^n - \left\{\int_0^{A-\delta} p_N(A)\,dA\right\}^n}{n\int_{A-\delta}^{A+\delta} p_N(A)\,dA} \qquad (9)$$

*Rice, on page 87 of Ref. 1, shows that this is only strictly true for a band-shape which resembles the Gaussian law, and for the bandwidth defined as that of the ideal filter (i.e., rectangular frequency response) giving the same output of noise power.

†In practice it is quite likely that δ will be a function of the amplitude A but this only affects the complexity of the integration and not the general argument.

1.3. *Display Saturating or Limiting, but J.N.Ds Zero*

Suppose now the display limits or saturates at an amplitude A_{sat} but that all j.n.ds are zero.

Amplitudes below A_{sat} will be unaffected and their contribution to detection can be found by integrating from 0 to A_{sat} instead of from 0 to ∞. Let this be ${}^{A_{sat}}_{0}\left[\mathbf{P}_D\right]$. However, there is a further contribution to detection when the signal-plus-noise peak exceeds A_{sat}. The probability of this occurrence is

$$\int_{A_{sat}}^{\infty} p_S(A)\,dA \qquad .. \quad (10)$$

If no noise peak exceeds this level we get positive detection.

If one noise peak exceeds this level we get one chance in two of obtaining correct detection.

If two noise peaks exceed this level we get one chance in three.

The probability of one noise peak is

$$\left[\int_{A_{sat}}^{\infty} p_N(A)\,dA\right]\left[\int_0^{A_{sat}} p_N(A)\,dA\right]^{n-2} \qquad .. \quad (11)$$

and by a similar argument to that used in Appendix 1.2 we can show that the total contribution to detection from 'signal peaks' above A_{sat} is

$$\left[\int_{A_{sat}}^{\infty} p_S(A)\,dA\right]\sum_{b=0}^{b=m}\frac{{}^mC_b}{b+1}\left[\int_{A_{sat}}^{\infty} p_N(A)\,dA\right]^b\left[\int_0^{A_{sat}} p_N(A)\,dA\right]^{m-b} \qquad .. \quad (12)$$

and again by the use of the expression derived in Appendix 3 we obtain

$$\mathbf{P}_{sat} = \frac{\int_{A_{sat}}^{\infty} p_S(A)\,dA}{n\int_{A_{sat}}^{\infty} p_N(A)\,dA}\left\{1-\left[\int_0^{A_{sat}} p_N(A)\,dA\right]^n\right\} \quad (13)$$

The total probability of detection is then

$$\mathbf{P} = {}^{A_{sat}}_{0}\left[\mathbf{P}_D\right] + \mathbf{P}_{sat} \qquad .. \quad .. \quad .. \quad (14)$$

1.4. *Display Saturating, with J.N.Ds Finite*

A similar argument can be used if the j.n.ds are finite, except that certain detection of a 'signal peak' above A_{sat} occurs only if the noise does not exceed $A_{sat}-\delta$. Hence the new expression is

$$\mathbf{P}_{sat} = \frac{\int_{A_{sat}}^{\infty} p_S(A)\,dA}{n\int_{A_{sat}-\delta}^{\infty} p_N(A)\,dA}\left\{1-\left[\int_0^{A_{sat}-\delta} p_N(A)\,dA\right]^n\right\} \quad (15)$$

1.5. *Effect of Contrast or Marking Threshold*

If the display does not mark below an amplitude A_m then if the 'signal peak' is below this no contribution is made to detection. This is taken into account by alteration of the lower limit of integration, e.g., in Appendix 1.1.

$$\mathbf{P}_D = \int_{A_m}^{\infty} p_S(A)\left[\int_0^{A} p_N(A)\,dA\right]^{n-1} dA \qquad .. \quad (16)$$

2. Probability of Detection in a Display Consisting of *R* Discrete Amplitude-Gates

When, instead of the display responding to the applied voltage or current in a continuous manner, it responds only with R discrete amplitude-intervals, determined by preset 'gates', detection of the 'signal peak' takes place by the following process:—

Let the signal-peak level lie between gates r and $r+1$, i.e., between amplitudes A_r and A_{r+1}. Then, in this range, detection is certain if no noise peak exceeds A_r, it is 0·5 if only one noise peak lies between A_r and A_{r+1}, it is $\frac{1}{3}$ if two noise peaks lie between A_r and A_{r+1}, and so on, and it is zero if any noise peaks rise above A_{r+1}. Clearly then the probability of detection when the signal is between amplitudes A_r and A_{r+1} is

$$P = \left[\int_{A_r}^{A_{r+1}} p_S(A)\,dA\right]\sum_{b=0}^{b=m}\frac{{}^mC_b}{b+1}\left[\int_{A_r}^{A_{r+1}} p_N(A)\,dA\right]^b\left[\int_0^{A_r} p_N(A)\,dA\right]^{m-b} \quad (17)$$

Hence the overall probability of detection is

$$\mathbf{P}_D = \sum_{r=1}^{r=R-1} P$$

$$= \sum_{r=1}^{r=R-1}\int_{A_r}^{A_{r+1}} p_S(A)\,dA\;\frac{\left\{\int_0^{A_{r+1}} p_N(A)\,dA\right\}^n-\left\{\int_0^{A_r} p_N(A)\,dA\right\}^n}{n\int_{A_r}^{A_{r+1}} p_N(A)\,dA} \quad (18)$$

3. Summation of Series in Appendix 1

$$\sum_{b=0}^{b=m}\frac{1}{b+1}\,{}^mC_b\,x^b\,y^{m-b}$$

$$= y^m\sum_{b=0}^{b=m}\frac{1}{b+1}\,{}^mC_b\left(\frac{x}{y}\right)^b$$

$$= \frac{y^{m+1}}{x}\sum_{b=0}^{b=m}\frac{1}{b+1}\,{}^mC_b\left(\frac{x}{y}\right)^{b+1}$$

$$= \frac{y^{m+1}}{x}\int_0^{x/y}\left(1+\frac{x}{y}\right)^m d\left(\frac{x}{y}\right)$$

$$= \frac{y^{m+1}}{x}\,\frac{\left(1+\frac{x}{y}\right)^{m+1}-1}{m+1}$$

$$= \frac{(x+y)^{m+1}-y^{m+1}}{(m+1)x}$$

$$= \frac{(x+y)^n-y^n}{nx} \text{ where } n = m+1$$

4. Accuracy of Simplified Probability Distributions

It is of interest to compare the properties of the simplified distributions (Fig. 3) assumed for the calculations, with those of the distributions derived by Rice[1] for the envelope of noise and signal-plus-noise when the r.m.s. input signal/noise ratio is approximately 2 dB. This condition is chosen so that both Rice's and the simplified distribution give the same value of a criterion R_{B1} used extensively for defining output signal/noise ratio in detection circuits. R_{B1} is defined as the ratio of the change of mean on application of the signal to the r.m.s. of the fluctuations. A fuller discussion of this and other criteria is given in Reference 2. Tables 3 and 4 compare the ratios of the mean, mean square and variance, and it can be seen that the simplified distribution is remarkably accurate in its reproduction of the essential parameters of the true distribution.

TABLE 3

Distributions as assumed in Figure 3

Distribution	Mean	Mean Square	Variance
Noise	5·33	34·67	6·22
Noise + Signal	8·33	80·33	10·89
Ratio	1·56	2·34	1·74

$$R_{B1} = \frac{\textit{Change in Mean}}{\sqrt{\textit{Variance}}} = \frac{3}{\sqrt{10}} = \underline{\underline{0{\cdot}9}}$$

TABLE 4

Distributions as defined by Rice for an input r.m.s. signal/noise ratio of 1·2 ($\simeq$ 2 dB)

Distribution	Mean	Mean Square	Variance
Noise	1·25	2	0·43
Noise + Signal	2·03	4·88	0·77
Ratio	1·63	2·44	1·79

$$R_{B1} = \frac{0{\cdot}78}{\sqrt{{\cdot}707}} = \underline{\underline{0{\cdot}89}}$$

STABILITY OF OSCILLATION IN VALVE GENERATORS

By A. S. Gladwin, Ph.D., D.Sc.

(*University of Sheffield*)

(*Concluded from p. 279, October issue*)

17. Other Stability Criteria

IN this Section some of the methods proposed by previous investigators are critically examined. Most writers, following Appleton and van der Pol[1,20], have postulated variations of amplitude and phase which are assumed to be so slow that terms in the variational equation containing time derivatives higher than the second could be neglected.

Now, in fact, the changes of amplitude and phase may be very rapid so that the fundamental assumption of the analysis is not always justified. Nevertheless the criteria so derived are valid for all cases of aperiodic instability however rapid the changes may be. The reason for this curious result lies in the fact, discussed in Section 13, that aperiodic stability is determined entirely by the behaviour of the characteristic function near to $p = 0$, and small values of p correspond to slow variations in the amplitude and frequency of oscillation.

Periodic instability is beyond the scope of these methods and various other proposals have been put forward. Edson[11] has suggested that Nyquist's criterion may be used to determine amplitude stability by interrupting the feedback network at some suitable point. A signal generator with a terminal voltage equal to that of the possible steady-state oscillation is connected across the grid side of the break, and across the other side is connected an impedance equal to that on the grid side. The steady voltage appearing across this impedance is equal to the signal-generator voltage.

If the applied voltage is now amplitude modulated the voltage returned to the other side of the break is also modulated but with a different magnitude and phase due to the action of the amplifier and feedback network. The complex ratio of the two modulations is analogous to the loop transmission function in feedback-amplifier theory and the oscillation should be stable if the locus of the ratio does not encircle the point 1, 0 when the modulation frequency is varied from $-\infty$ to ∞.

It was shown in Section 7 that the use of this contour leads to difficulties, the appropriate one being that of Fig. 7. Another point is that if low-frequency currents flow from terminals 1 to 2 of Fig. 1 it may be impossible to interrupt the network without destroying the relations between the low-frequency currents and voltages. This difficulty can be avoided in the following way. A generator of zero impedance is inserted in any branch of the network, its e.m.f. being such that, when added to the steady oscillation, the result is an amplitude-modulated wave. The current of oscillation frequency flowing through the generator is similarly modulated, and the complex ratio of the modulations of voltage and current defines the impedance into which the generator operates. Stability is obtained if the locus of this impedance does not enclose the origin. This is equivalent to the closed-circuit form of Nyquist's criterion[25].

It is convenient to consider the more general case in which the generator e.m.f. represents modulations of amplitude, of frequency, and of

the mean grid voltage. Let a generator of e.m.f. $e = V_d \sum_{-1}^{1} m_n \exp.\,(p + jn\omega_0)\,t$ be inserted in the lead between the grid and terminal 2 in Fig. 1. The calculation proceeds on the lines of Section 6 with $v_{gd} - e$ written in place of v_{gd} in the expressions for i_{ad} and v_{ad}. Since only symmetrical networks can be treated by this method, $q = 1$ and $Z_t^- = Z_t^+$, $c_{-1} = a_1$, etc. The equations (6.2) for u_1, u_0 and u_{-1} become

$$\begin{bmatrix} a_1 & b_1 & c_1 \\ a_0 & b_0 & a_0 \\ c_1 & b_1 & a_1 \end{bmatrix} \begin{bmatrix} u_1 \\ u_0 \\ u_{-1} \end{bmatrix} = \begin{bmatrix} h_1 \\ h_0 \\ h_{-1} \end{bmatrix} \qquad \ldots \quad \ldots \quad (17.1)$$

where

$$\left.\begin{aligned} h_1 &= m_1\,(1 + G_0 Z_i^+/\mu) + m_0 G_1 Z_t^+ Z_i^0/\mu Z_t^0 + m_{-1}(G_2 Z_i^+/\mu \\ h_0 &= m_0\,(1 + G_0 Z_i^0/\mu) + (m_1 + m_{-1})\,G_1 Z_t^0 Z_i^+/\mu Z_t^+ \\ h_{-1} &= m_{-1}(1 + G_0 Z_i^+/\mu) + m_0 G_1 Z_t^+ Z_i^0/\mu Z_t^0 + m_1 G_2 Z_i^+/\mu \end{aligned}\right\} \qquad \ldots \quad (17.2)$$

If $m_1 = m_{-1} = 1$ and $m_0 = 0$ the sum of the real part of e and the steady oscillation is an amplitude-modulated wave. In calculating the impedance into which the generator operates it is sufficient, by virtue of symmetry, to consider the voltage and current at only one of the high frequencies, say $p + j\omega_0$. Equation (17.1) can be solved in the usual way for u_1, u_0 and u_{-1} and the grid current of frequency $p + j\omega_0$ can then be calculated from (5.3) and (5.4). The impedance is given by the ratio of $V_d \exp.\,(p + j\omega_0)\,t$ to this current, and is

$$Z = A\,(p)/M\,(p) \qquad \ldots \quad \ldots \quad \ldots \quad (17.3)$$

where $A\,(p)$ is the amplitude-stability function of Section 8 and

$$M\,(p) = (S_0 + S_2)(h_1 b_0 - h_0 b_1) + S_1\,\{h_0\,(a_1 + c_1) - 2h_1 a_0\} \qquad \ldots \quad (17.4)$$

Now the amplitude is unstable or stable as the locus of $A\,(p)$ does or does not enclose the origin. If the locus of Z is to be a true criterion of stability it must enclose the origin the same number of times and in the same sense as that of $A\,(p)$. It follows that the locus of $M\,(p)$ must not enclose the origin. The simplified case of $\mu = \infty$ is first considered. Substituting for h_1, a_1, etc., according to (17.2) and (6.3),

$$M\,(p) = S_0 + S_2 + \{S_0\,(S_0 + S_2) - 2S_1^2\}Z_0^0 + [G_0\,(S_0 + S_2) - 2G_1 S_1 - k\,\{S_0\,(S_0 + S_2) - 2S_1^2\}]\,Z_t^0$$

The impedances Z_0^0 and Z_t^0 are passive driving-point and transfer functions and thus can have no poles in the right-hand half-plane. Only zeros of $M\,(p)$ need therefore be considered. (5.6) shows that $S_0 + S_2$ and $S_0\,(S_0 + S_2) - 2S_1^2$ are always positive. Also, since Z_0^0 is a passive driving point impedance, its real part is always positive. However, there is nothing to prevent the coefficient of Z_t^0 from being negative, and the real part of Z_t^0 may itself be negative. Hence it is possible for $M\,(p)$ to have a zero in the right-hand half-plane. A necessary and sufficient condition for $M\,(p)$ not to enclose the origin is therefore $Z_t^0 \equiv 0$. This ensures that the real part of $M\,(p)$ is always positive.

For the general case where μ is finite the application of this condition gives

$$M\,(p) = (1 + G_0 Z_i^0/\mu)\,\{1 + (G_0 + G_2)\,Z_i^+/\mu\} \times [S_0 + S_2 + \{S_0\,(S_0 + S_2) - 2S_1^2\}Z_0^0]$$

(5.15) shows that G_0 and $G_0 + G_2$ are always positive. Z_i^0 and Z_i^+ are passive driving-point functions and so have positive real parts. Hence the loci of none of the three factors in this expression can enclose the origin and so neither can that of $M\,(p)$. The condition $Z_t^0 \equiv 0$ means that low-frequency currents cannot be transmitted through the network. When this condition is satisfied it is possible to select a point where the network may be interrupted to apply the open-circuit form of the Nyquist test in the manner proposed by Edson. The results are the same as for the closed-circuit test.

In the foregoing analysis the stability rule was expressed in terms of the high-frequency components of voltage and current, but Edson has suggested[14] that the Nyquist open- and closed-circuit tests may be used also at low frequencies. This method, if valid, would be most valuable, for it could be applied also to asymmetrical networks. It will be sufficient to examine the simplest case of the closed-circuit form of test with a symmetrical network and with $\mu = \infty$.

The generator e.m.f. is now $e = V_d \exp.\,pt$; i.e., $m_1 = m_{-1} = 0$ and $m_0 = 1$. The impedance into which the generator operates is the ratio of e to the grid current of frequency p. It is calculated in the same way as before and is $Z = A\,(p)/L\,(p)$, where $A\,(p)$ is the amplitude stability function and

$$L\,(p) = S_0 + \{S_0\,(S_0 + S_2) - 2S_1^2\}\,Z_0^+ + [S_0\,(G_0 + G_2) - 2S_1 G_1 - k\,\{S_0\,(S_0 + S_2) - 2S_1^2\}]Z_t^+$$

For the impedance locus to be a valid criterion of amplitude stability $L\,(p)$ must not enclose the origin. S_0 and the real part of the first term are always positive, but the coefficient of Z_t^+ may be positive or negative. The necessary and sufficient condition for $L\,(p)$ not to enclose the origin is that $Z_t^+ \equiv 0$, but this implies that there is no transmission of high-frequency current through the network and therefore no oscillation. It follows that stability cannot be determined by applying the Nyquist test at low frequencies.

Although Edson was concerned only with

amplitude stability his method may be adapted to determine also frequency stability in symmetrical networks. Considering the closed-circuit form of test, let $-m_{-1} = m_1 = 1$ and $m_0 = 0$. The sum of the real part of e and the steady oscillation is then a frequency-modulated wave. The impedance into which the test generator operates is taken as the ratio of voltage to current at the frequency $p + j\omega_0$ and is $Z = F(p)/N(p)$, where $F(p)$ is the frequency stability function of (8.2) and $N(p) = (1 - Z_i^+/\mu R_E)/r_g$. Since R_E is negative and Z_i^+ has a positive real part the locus of $N(p)$ cannot enclose the origin, and the locus of Z therefore makes the same number of encirclements as that of $F(p)$. Both the open- and closed-circuit forms of the Nyquist test may be used without restriction to determine frequency stability.

Other criteria for periodic amplitude stability proposed by Edson and by van Slooten are examined in the next Section.

18. Experimental Results and Conclusions

A series of tests was carried out to check the main points of the theory. Two amplifiers—a triode and a pentode—were used of which the parameters occurring in expressions (4.4), (4.19), (4.22) and (4.23) were as shown in Table 1.

TABLE 1

Amplifier	g (mhos)	V_{ca} (volts)	μ	k
1	$6{\cdot}57 \times 10^{-3}$	$-8{\cdot}10$	20·6	1
2	$6{\cdot}40 \times 10^{-3}$	$-2{\cdot}70$	2200	0·78
	b_g (mhos)	V_{cg} (volts)	I_0 (amps)	V_0 (volts)
1	$1{\cdot}05 \times 10^{-3}$	0·05	$1{\cdot}27 \times 10^{-4}$	0·103
2	$1{\cdot}98 \times 10^{-3}$	$-0{\cdot}16$	$9{\cdot}9 \times 10^{-4}$	0·105

These figures were obtained from plots of the anode and grid currents. At small values of i_a the three-halves law is not followed, and for small values of v_g the grid-current curve is not linear. V_{ca} and V_{cg} were therefore found by extrapolating the linear parts of the i_g and $i_a^{2/3}$ graphs. I_0 and V_0 were obtained in a similar way. The effects of departures from the theoretical forms are discussed later.

Dust-cored coils were used to obtain a high coupling factor between the two windings. This makes the voltage ratio between anode and grid equal to $-R_i/R_t = -R_I/R_T$, and also $R_n = 0$. The inductance of the main coil was 1·015 mH. Unless otherwise stated, the oscillation frequency was 50·76 kc/s.

Test 1. *Oscillation Amplitude.* (*Section* 4)

For tests (b) and (c) (Table 2) the circuit of Fig. 12 was used with $R_a = 0$; for test (a) the same but with the anti-resonant circuit and the coupling coil interchanged. The oscillation amplitude was varied by adjusting the resistance R and the number of turns of the coupling coil. Amplifier 1 was used throughout. The method of calculation is described in Section 4.

TABLE 2

Test	R (kΩ)	N	V_{g1} (volts) Calc.	V_{g1} (volts) Meas.
(a) $K = 0{\cdot}75$	2·09	2·32	8·90	8·80
$R_g = 17{\cdot}5$ kΩ	4·57	4·23	18·0	18·0
$-R_I/R_T = 0{\cdot}205$	6·90	5·50	27·3	25·5
	12·5	7·52	—	39·6
(b) $K = 1{\cdot}00$	1·06	2·49	7·50	7·40
$R_g = 66{\cdot}6$ kΩ	2·09	4·86	12·4	12·7
$-R_I/R_T = 2{\cdot}44$	4·57	10·3	20·9	21·1
	6·90	15·2	27·2	26·7
(c) $K = 1{\cdot}83$	6·89	2·44	6·48	6·22
$R_g = 614$ kΩ	12·5	4·43	8·40	7·78
$-R_I/R_T = 9{\cdot}75$	27·7	9·76	10·4	9·76

With the exception of the last result of test (a) the calculated and measured amplitudes agree within the limits of experimental error. According to Fig. 3 there is no value of Y corresponding to $N = 7{\cdot}52$ and $K = 0{\cdot}75$. Departures from the three-halves law at small values of i_a would produce only slight errors unless the valve had an exceptionally long 'tail'. However, for large positive grid voltages the anode current may be much less than the theoretical value. This would account for the last result of test (a), for the maximum grid voltage there is 10·2 volts. The slightly higher errors in test (c) may be attributed to the fact that quantity $1 + R_I/\mu R_T$, which is the denominator of K, is approximately 0·5, so that in calculating K any errors in R_I/R_T and μ are doubled.

Departures of the grid-current law from the semi-linear form at small voltages produce usually little error. When R_g is small the grid is driven well into the linear region unless the oscillation amplitude is very small. If V_{g1} is excessively large the grid may be driven beyond the linear region. The effective value of b_g and thus of K is then increased. When R_g is large the ratio V_g/V_{g1} is almost -1 and is practically independent of changes in the value of b_g.

Test 2. *Frequency Stability.* (*Section* 9)

The circuit used was a modification of that shown in Fig. 10. Three identical coils were used with equal shunt resistances, the effect of varying the shunt resistance nR of the central coil being simulated by a potentiometer connected across the coupling coil. With $\mu = \infty$ and a large grid-leak resistance, the equation for the modified

circuit is the same as for the original, n being now the potentiometer ratio. The circuits were tuned to frequencies of 45, 50 and 55 kc/s; i.e., $\omega_m/\omega_0 = 0{\cdot}1$. Starting with the potentiometer set at maximum ($n = 1$) and the oscillation frequency at 50 kc/s, the setting was reduced to the critical value at which instability began.

TABLE 3

Q	c	n Calc.	n Meas.
10	2	0·40	0·38
15	3	0·70	0·66
20	4.	0·82	0·79

The theoretical values of n were calculated from (9.11) and (9.5). This theory is strictly valid only when Q is very large and ω_m/ω_0 very small. It may be shown that the true theoretical value of n is less than that of the approximate theory and that, with the values of parameters used in the experiment, the difference is of the same order as the observed error.

At the critical value of n instability began as a small sustained frequency modulation. As n was further decreased the oscillation frequency changed suddenly to a new stable value.

Test 3. *Amplitude Stability–Hysteresis.* (*Section* 10)

The circuit was that of Fig. 12 with $R_a = 0$. Instability of the first kind—a change from one large amplitude to another—could not be detected with Amplifier 1. Using Amplifier 2 it was produced by lowering the screen voltage (normally 150) to 10 V, and making $R_g = 5{\cdot}43\,\text{k}\Omega$. The critical amplitude corresponded to $V_g = -0{\cdot}45$ V. At such low voltages the parameters b_a, etc., have little or no meaning, and the confirmation is thus only qualitative. In all practical amplifiers this form of instability is inhibited by the departure from the three-halves law at large grid voltages.

For the second type of hysteresis effect—the sudden starting and stopping of oscillation—the anti-resonant circuit and coupling coil in Fig. 12 were interchanged. The resistance R was adjusted till oscillation just began. This was done for various values of R_g to find the critical value at which hysteresis appeared. From the measured value of R_g the quantities Y, r_g, R_E and V_g/V_0 can be found by using (4.24), (5.16) and Fig. 4. The stability criterion (10.8) can then be used to calculate the ratio $R_\theta/R_T = R_T/R_I$. Amplifier 1 was used with $R_a = 0$.

TABLE 4

R_g ($k\Omega$)	V_g/V_0	Y	$-R_\theta/R_T$ Calc.	$-R_\theta/R_T$ Meas.
500	− 4·84	0·061	9·8	9·8
300	− 4·42	0·056	6·5	4·9

It is a matter of some difficulty to decide whether or not a hysteresis effect exists, for at the critical value of R_g the initial stable amplitude is vanishingly small, and it is not easy to distinguish between a small hysteresis effect and a smooth start of oscillation. The first result was obtained by taking the average of the two values of R_g at which it was certain that hysteresis did and did not exist. The second result is a single estimation of R_g.

Test 4. *Periodic Amplitude Instability.* (*Section* 11)

The circuit of Fig. 12 was used with $R_a = 0$. For various values of R and R_g the grid capacitance C_g was increased until instability set in. To restore stability C_g had often to be reduced to a value less than the original critical value.

Using the measured values of R, R_g and V_g, the values of S_0R_g, S_2r_g and G_2R_E are obtained from Figs. 2, 5 and 6. The stability criterion (11.8) can then be used to calculate the critical value of C_g. Amplifier 1 was used and $-R_I/R_T = 2{\cdot}44$.

With the exception of the last result in Test (a) (Table 5), the calculated and measured values of C_g agree well. The error is probably connected with the large value (8 V) of the maximum grid voltage. Departures of the grid-current law from the semi-linear form produce errors in S_0 and S_2 which are likely to be serious for large values of R_g and small values of V_{g1}, for the grid is then

TABLE 5

Test	R (kΩ)	$-V_g$ (volts)	Q	C_g (μF × 10 ^{3}) Calc.	Meas.	van S.	Edson
(a)	1·15	6·60	3·55	∞	∞	∞	0·75
	2·09	12·2	6·47	11·3	11·8	30·0	1·4
R_g = 23·1 kΩ	4·57	22·0	14·2	9·40	10·5	23·6	3·0
	6·90	28·8	21·3	10·5	13·2	27·0	4·5
(b)	1·06	6·46	3·27	∞	∞	∞	0·27
	2·09	11·2	6·47	8·00	8·31	22·7	0·54
R_g = 66·6 kΩ	4·57	18·5	14·2	6·50	6·50	16·4	1·2
	6·90	23·6	21·3	6·95	6·85	17·5	1·8
(c)	0·99	6·60	3·06	61·0	∞	∞	0·09
	2·09	10·7	6·47	5·55	5·49	17·2	0·20
R_g = 194 kΩ	6·90	20·3	21·3	5·20	5·36	12·9	0·65
	12·5	27·5	38·6	4·82	4·97	15·5	1·2

driven only slightly positive. Errors must also be expected with small values of R_g and large values of V_{g1}.

The last two columns in Table 5 are calculated from formulae given by van Slooten[9] and Edson[15]. Van Slooten's criterion is

$$1{\cdot}4Q\,(b_gR_g)^{2/3}\frac{X_g}{R_g} > \frac{Y-1}{1-Y\,(1+V_{g1}/V_g)}$$

Edson's criterion is $2QX_g/R_g > -V_{g1}/V_g$.

In each test the first result gives the maximum amplitude for which stability is independent of C_g. In van Slooten's theory all values of $-V_g$ less than $-V_{ca}$ (8·1 V in this case) represent stable states.

Test 5. Periodic Amplitude Stability with Fixed Grid Bias. (*Section* 11)

The circuit used was that of Fig. 12 with the grid leak replaced by a source of e.m.f. sufficient to stop grid current. The h.t. supply voltage was adjusted to keep the mean anode voltage at its normal value of 150 V. With all other parameters fixed, the decoupling capacitance C_a was adjusted to the point of instability.

Using the measured values of R, R_a, V_g and V_{g1} a value for C_a can be calculated from (11.11) by way of Fig. 6, (5.14), etc. Amplifier 1 was used and $-R_I/R_T = 2{\cdot}44$.

TABLE 6

R_a (kΩ)	R (kΩ)	$-V_g$ (volts)	V_{g1} (volts)	Q	C_a (μF × 10^{-3}) Calc.	Meas.
19·8	1·22	7·00	5·55	3·78	22·7	14·1
19·8	1·71	8·00	5·87	5·30	10·5	8·6
11·4	1·50	7·50	5·23	4·65	18·9	14·2

This experiment was difficult to carry out because the oscillation amplitude changes very rapidly with variations of R and V_g. Another source of error lies in the fact that the value of C_a is about the same as that of the tuning capacitance C and that Q is small. This means that the impedance of C_a at the oscillation frequency is not negligible compared with R as assumed in the theory.

Test 6. Periodic Amplitude Stability with three Time Constants. (*Section* 12)

The circuit of Fig. 12 was used with amplifier 1, the h.t. supply voltage being adjusted to keep the mean anode voltage constant. For various values of R_a and R_g the value of C_g was adjusted to the unstable point. The other parameters, which were constant throughout, were $R = 2{\cdot}09$ kΩ, $C_a = 0{\cdot}00905$ μF, $Q = 6{\cdot}47$, $-R_I/R_T = 2{\cdot}44$.

Using the measured values of V_g, values for C_g can be calculated from (11.6), (11.7) and (12.2) as described in Section 12.

TABLE 7

R_g (kΩ)	R_a (kΩ)	$-V_g$ (volts)	C_g (μF × 10^{-3}) Calc.	Meas.
23·1	0	12·2	11·3	11·8
	2·14		18·1	18·1
	4·83		25·9	24·8
66·6	0	11·2	8·0	8·3
	2·14		12·7	13·5
	4·83		17·5	17·9
194	0	10·7	5·60	5·50
	2·14		8·70	8·50

The value of 0·00905 μF for C_a is much less than would normally be used, being in fact about equal to the tuning capacitance C. This value was chosen in order to demonstrate clearly the effect of the decoupling network. With values of C_a which would be used in practice the effect on the critical value of C_g was too small to be measured accurately.

Test 7. Hartley Oscillator. (*Section* 12)

Fig. 13 shows the circuit used. For the first two tests R_a was fixed and C_g adjusted to the critical value, and in the last two C_g was fixed (at ∞) and R_a was varied. The other parameters, which were fixed throughout, were $R_g = 53{\cdot}1$ kΩ, $R = 4{\cdot}57$ kΩ, $Q = 14{\cdot}2$, $-V_g = 8{\cdot}4$ V, $C_a = 0{\cdot}0585$ μF, $-R_I/R_T = 2{\cdot}44$. Amplifier 2 was used.

The values of C_g were calculated from $a_1a_2 = a_0a_3$, and those of R_a from $a_2 = 0$, $a_1 = 0$, using the expressions for a_0, etc. given by (12.4).

TABLE 8

R_a (kΩ) Meas.	Calc.	C_g (μF × 10^{-3}) Calc.	Meas.
0	—	8·82	9·74
1·00	—	26·4	29·5
1·59	1·68	—	∞
5·66	4·25	—	∞

In accordance with the ideas put forward in Section 12 there is a range of values of R_a over which the amplitude is stable when $C_g = \infty$. When the values of R_a, C_a and C_g are compared with those of the previous test the powerful stabilizing effect of the degenerative feedback at low frequencies becomes evident. A similar effect could be obtained with the circuit of Fig. 12

if the lower terminal of C_g were connected to the upper terminal of C_a instead of to the cathode.

The errors are somewhat larger than in previous experiments but the reason for this was not discovered.

Test 8. *Frequency Hysteresis.* (*Section* 14)

The circuit of Fig. 14 was used with amplifier 2. Grid bias was obtained by grid leak and capacitor, the damping resistance R being adjusted to suit. The mutual inductance was realized by using a third coil. After M and R had been set to suitable values the secondary tuning capacitance C_s was varied and the frequencies of the various critical points in Fig. 15 were measured. Owing to the rapid variation of frequency with C_s it was not possible to find the frequencies at 'a' and 'c'. The values of C_s at 'b' and 'd' were also measured, but no values could be found corresponding to 'f' and 'g' because of the extreme flatness of the maximum and minimum.

$R = 6{\cdot}7$ kΩ, $b = M/L = 0{\cdot}1$, $C = 9{,}800\ \mu\mu$F

With $M = 0$, oscillation frequency $= 48{\cdot}50$ kc/s.

$Q = 20$

From (14.1), $u = 3$.

From (14.3), values of sQ at points 'b' and 'd' are $\pm\ 1{\cdot}18$

Hence values of C_s at points 'b' and 'd' are $9{,}800 \pm 580\ \mu\mu$F

Measured values $= 9{,}800 \pm 600\ \mu\mu$F

From (14.5) frequencies at points 'b' and 'd' are $48{\cdot}50 \pm 1{\cdot}65$ kc/s

Measured values $= 48{\cdot}50 \pm 1{\cdot}66$ kc/s

From (14.7) frequencies at points 'f' and 'g' are $48{\cdot}50 \pm 2{\cdot}43$ kc/s

Measured values $= 48{\cdot}50 \pm 2{\cdot}49$ kc/s

Test 9. *Aperiodic Stability with Asymmetrical Network.* (*Section* 14)

Fig. 16 shows the circuit used. With R_a fixed R was adjusted till oscillation just began and it was observed whether or not a hysteresis effect was present. This was repeated for different values of R_g to find the value of R at which hysteresis was just detectable. Amplifier 2 was used and $b = -M/L = 0{\cdot}205$. With $R_g =$ 349 kΩ the critical value of R was 3·92 kΩ.

Using (4.24), (5.8), (5.16), (14.10) and Fig. 4, the quantity P_a given by (14.8) is found to be 0·16. P_a is also the l.h.s. of the stability criterion (14.12). Using the above figures the r.h.s. of this inequality is found to be 0·18. The discrepancy may be attributed to the experimental difficulty of deciding if a hysteresis effect exists.

Test 10. *Effect of R_a on Oscillation Amplitude.* (*Appendix* 3)

The circuit of Fig. 12 was used, the h.t. supply voltage being kept constant while R_a was varied. The other parameters were $R = 2{\cdot}09$ kΩ, $R_g =$ 66·6 kΩ, $-R_I/R_T = 2{\cdot}44$. Values of the oscillation amplitude were calculated from (A3.2) and Fig. 17. Amplifier 1 was used.

TABLE 9

R_g (kΩ)	V_{g1} (volts) Calc.	V_{g1} (volts) Meas.
0	12·4	12·7
4·83	9·50	9·20
11·4	6·85	7·07
19·8	5·43	5·37

These experiments have shown that the theory, so far as it goes, is substantially correct. Errors arise mainly when the actual behaviour of the amplifier and network depart from the assumed forms. It seems safe to say that the general theory is always valid provided the true values of the various parameters are used.

From the practical point of view a serious drawback is that the stability criteria are valid only for small disturbances whereas, to be of any practical use, an oscillator must have stability under all conditions of operation which may include large switching surges. A theory to take account of large disturbances would need to be a non-linear theory, in contrast to the linear theory of this paper. Such a theory would be very complicated and each particular oscillator would have to be treated as a separate problem.

A second disadvantage is that the stability criteria are not very simple: it would often be quicker to find the solution by experiment. However, it must be remembered that the analysis has been carried out in detail with the object of testing as accurately as possible the basic theory. Such refinements would not be justified in practical design calculations, for the primary data would seldom be known with any great accuracy.

APPENDIX 1

The Steady-State Oscillation

Let the grid-current characteristic have the semi-linear form $i_g = e\,(v_g) = b_g\,(v_g - V_{cg})$ when $v_g > V_{cg}$

$= 0 \qquad v_g \leqslant V_{cg}$ (A1.1)

b_g and V_{cg} are parameters of the valve.

Let $v_g = V_{g1} \cos \omega_0 t + V_g$ .. .. (A1.2)

It is assumed that current flows during only part of each cycle. The conduction angle 2ϕ is defined by

$\cos \phi = (V_{cg} - V_g)/V_{g1}$ .. .. (A1.3)

If V_{g1} is constant V_g and ϕ vary with V_{g2}. Let ϕ_0 be the value of ϕ when $V_{cg} = 0$, and let $\phi = \phi_0 + \phi_1$. If ϕ_1 is so small that $\cos \phi_1 = 1$, $\sin \phi_1 = \phi_1$ it follows from (4.2) and the above equations that

$$1 = (\tan\phi_0 - \phi_0)\, b_g R_g/\pi$$
$$\phi = \phi_0\,(1 - \pi V_{cg}\cot\phi_0/b_g R_g V_{g1}\phi_0 \sin\phi_0)$$
$$1 - V_{cg}\sec\phi/V_{g1} = (\tan\phi - \phi)\, b_g R_g/\pi$$
$$V_g = -\cos\phi_0\,(V_{g1} - V_{cg}\phi_0/\sin\phi_0) \qquad \text{(A1.4)}$$

The first equation gives ϕ_0 in terms of $b_g R_g$. ϕ and V_g follow from the others. As $b_g R_g$ varies from 10 to 1000 the coefficient of V_{cg}/V_{g1} in the second equation varies from 0·40 to 0·34, and $\phi_0/\sin\phi_0$ in the fourth equation varies from 1·13 to 1. Since V_{cg}/V_{g1} is always small in practice it is sufficiently accurate to take average values at say $b_g R_g = 100$ namely, 0·36 and 1. This approximation gives

$$\left.\begin{aligned} \phi &= \phi_0\,(1 - 0{\cdot}36\,V_{cg}/V_{g1}) \\ V_g &= V_g'\,(1 - V_{cg}/V_{g1}) \\ \text{where } V_g' &= -V_{g1}\cos\phi_0 \end{aligned}\right\} \qquad \text{(A1.5)}$$

Using the first equation of (A1.4) $-V_g'/V_{g1}$ can be found as a function of $b_g R_g$ (Fig. 2).

The grid input resistance is found from (4.3), (A1.1) and (A1.3) as $r_g = -R_g\,(V_{g1}/V_g)\,(\sin\phi - \phi\cos\phi)/(\phi - \sin\phi\cos\phi)$. Using the value of ϕ given by (A1.3) it can be shown that the fractional error produced by writing ϕ_0 for ϕ in this equation is of the order $0{\cdot}07\phi^2 V_{cg}/V_{g1}$ which is negligible. Substituting for V_{g1}/V_g according to (A1.5) gives $r_g = r_g'\,(1 + V_{cg}/V_{g1})$ where $r_g' = R_g\,(\sin\phi_0 - \phi_0\cos\phi_0)/\cos\phi_0\,(\phi_0 - \sin\phi_0\cos\phi_0)$. Using (A1.4) r_g'/R_g can be calculated as a function of $b_g R_g$ (Fig. 2).

When V_g/V_{g1} is known, the oscillation amplitude could be found by solving equation (4.13) to obtain Y in terms of K and N. An easier method is to make use of the relation between N and $G_0 - G_2$ (5.14) namely $G_0 - G_2 = g/N$. When the valve operates in the space-charge-limited condition the anode current (in the absence of grid current) follows the three-halves law

$$\begin{aligned} f(v) &= b_a v^{3/2} \quad v > 0 \\ &= 0 \quad\quad\; v < 0 \end{aligned} \qquad \text{(A1.6)}$$

and $v = V_e\cos(\omega_0 t + \theta) + V_g - V_{ca}$

In the following Appendix the values of G_0 and G_2 corresponding to this state are found in terms of the parameter $H = 1 - K + K/Y$. Using these values N can be expressed as follows.

If $H > 2$

$$1/N = (8/15\pi)\,(HY/K)^{\frac12}\,[\{3 + (H-1)^2\}\,E - (H-1)(H-2)\,F] \qquad \text{(A1.7)}$$

where F and E are the complete elliptic integrals of the first and second kinds. In the usual notation

$$F = F_1\,(k, \tfrac12\pi),\; E = E_1\,(k, \tfrac12\pi) \text{ where } k = (2/H)^{\frac12} \qquad \text{(A1.8)}$$

When $H < 2$

$$1/N = (4/15\pi)\,(2Y/K)^{\frac12}\,[\{6 + 2\,(H-1)^2\}\,E - (H-2)(H-4)\,F] \qquad \text{(A1.9)}$$

$$F = F_1\,(k', \tfrac12\pi),\; E = E_1\,(k', \tfrac12\pi) \text{ where } k' = (H/2)^{\frac12} \qquad \text{(A1.10)}$$

N can thus be calculated as a function of K and Y (Fig. 3). When $Y \to 0$, $H \to K/Y$ and it can be shown from (A1.7) that $N \to 1$. When $Y \to \infty$, $H \to 1 - K$ and, since a negative value for H is inadmissible, Y must be finite for all values of N when $K > 1$. When $K < 1$ it is evident from (A1.9) that as $Y \to \infty$ then $N \to 0$.

For small values of grid voltage and when the effects of grid emission and ionization can be neglected, the grid current is approximately

$$i_g = e\,(v_g) = I_0\,\exp.\,(v_g/V_0) \qquad \text{(A1.11)}$$

where I_0 and V_0 are constants of the valve. Equation (4.2) then gives $V_g = -I_0 R_g\,\exp.\,(V_g/V_0)\,B_0(V_{g1}/V_0)$ and (4.3) gives $r_g = -\frac12 R_g\,(V_{g1}/V_g)\,B_0(V_{g1}/V_0)/B_1(V_{g1}/V_0)$. In these expressions B_0 and B_1 are the modified Bessel functions of the first kind (usually denoted by I_0 and I_1). If V_{g1} is small these functions can be replaced by the first two terms of their series expansions $B_n(x) = (\frac12 x)^n\,\{1 + x^2/4\,(n+1)\}/n!$. Then as $V_{g1} \to 0$

$$V_g = -I_0 R_g\,\exp.\,(V_g/V_0),\; r_g = -R_g V_0/V_g \qquad \text{(A1.12)}$$

Since I_0 and V_0 are known V_g/V_0 can be found as a function of $I_0 R_g/V_0$. (Fig. 4.)

The rates of change of V_g and r_g with V_{g1} are also required. Using the above approximations for the Bessel functions it is easily shown that as $V_{g1} \to 0$

$$dV_g/dV_{g1} = nV_{g1}/V_g,\; dr_g/dV_{g1} = mr_g V_{g1}/V_g^2 \qquad \text{(A1.13)}$$

$$\left.\begin{aligned} \text{where } n &= (V_g/V_0)^2/2\,(1 - V_g/V_0) \\ m &= -(V_g/V_0)^3\,(1 + V_g/V_0)/4\,(1 - V_g/V_0) \end{aligned}\right\} \qquad \text{(A1.14)}$$

APPENDIX 2

Evaluation of S_n and G_n

Let the grid current have the semi-linear form of (A1.1)

$$\begin{aligned} \text{Then } e'(v_g) &= b_g \text{ when } v_g > V_{cg} \\ &= 0 \quad\quad\; v_g < V_{cg} \end{aligned}$$

From the definition (5.1) of S_n, $S_0 = b_g\phi/\pi$, $S_1 = b_g\sin\phi/\pi$, $S_2 = b_g\sin 2\phi/2\pi$. Using expressions (A1.5) $S_0 R_g = S_0' R_g\,(1 - 0{\cdot}36\,V_{cg}/V_{g1})$ where $S_0' R_g = b_g R_g\phi_0/\pi$ $S_2/(S_0 - S_2) = S_2 r_g = S_2' r_g\,(1 + 0{\cdot}72\,V_{cg}/V_{g1})$ where $S_2' r_g = \sin 2\phi_0/(2\phi_0 - \sin 2\phi_0)$. Also $S_2/S_1 = \cos\phi = -(1 - V_{cg}/V_{g1})\,V_g'/V_{g1} + V_{cg}/V_{g1}$. Using the first equation of (A1.4), ϕ_0 and thence $S_2' r_g$ and $S_0' R_g$ can be calculated as functions of $b_g R_g$ (Fig. 5).

When $f(v)$ follows the three-halves law of (A1.6)

$$\begin{aligned} f'(v) &= 1\tfrac12 b_a v^{\frac12} \quad v > 0 \\ &= 0 \quad\quad\; v < 0 \end{aligned}$$

Putting $g = 1\frac12 b_a\,(-V_{ca})^{\frac12}$ the definition of G_n (5.10) becomes $G_n = (g/\pi)\int_0^\theta \{1 - Y + (Y/K)\cos x\}^{\frac12}\cos nx\,dx$

where $\theta = \pi$ if $Y < K/(1+K)$, and $\cos\theta = K\,(1 - 1/Y)$ if $Y > K/(1+K)$. Writing $H = 1 - K + K/Y$, the integral becomes

$$G_n = (2g/\pi)\,(HY/K)^{\frac12}\int_0^{\frac12\theta}\{1 - (2/H)\sin^2 x\}^{\frac12}\cos 2nx\,dx \qquad \text{(A2.1)}$$

If $H > 2$, $\theta = \pi$, and if $H < 2$ the transformation $\sin y = (H/2)^{\frac12}\sin x$ makes the upper limit of integration again $\frac12\pi$. In both cases the result can be expressed in terms of the complete elliptic integrals.

$$\begin{aligned} \text{If } H > 2,\; G_0 &= (2g/\pi)\,(HY/K)^{\frac12}E \\ G_1 &= (2g/3\pi)\,(HY/K)^{\frac12}\,\{(H-1)\,E - (H-2)F\} \\ G_2 &= (2g/15\pi)(HY/K)^{\frac12}[\{3 - 4(H-1)^2\}\,E \\ &\quad + 4\,(H-1)\,(H-2)\,F] \end{aligned} \qquad \text{(A2.2)}$$

where F and E are given by (A1.8)

$$\begin{aligned} \text{If } H < 2,\; G_0 &= (g/\pi)\,(2Y/K)^{\frac12}\,\{2E + (H-2)\,F\} \\ G_1 &= (g/3\pi)\,(2Y/K)^{\frac12}\,\{2\,(H-1)\,E - (H-2)F\} \\ G_2 &= (g/15\pi)(2Y/K)^{\frac12}\{[6 - 8\,(H-1)^2]\,E \\ &\quad + (H-2)\,(4H-1)\,F\} \end{aligned} \qquad \text{(A2.3)}$$

where F and E are given by (A1.10)

The following approximations are obtained from power series expansions of F and E. When V_{g1} is very small and V_g does not tend to zero with V_{g1} (e.g., exponential grid-current law), K and H are large, and then

$$\begin{aligned} G_0 = g\,(1 - Y)^{\frac12} &= -1/R_K,\; G_1 = -Y/4K\,(1 - Y)R_K \\ G_2 &= Y^2/32K^2\,(1 - Y)^2 R_K \end{aligned} \qquad \text{(A2.4)}$$

$$\begin{aligned} \text{When } H < 2,\; G_0 &= \tfrac12 g\,(Y/2K)^{\frac12}H\,(1 + H/16 + 3H^2/256\,..) \\ G_1 &= \tfrac12 g\,(Y/2K)^{\frac12}H\,(1 - 3H/16 - 5H^2/256\,..) \\ G_2 &= \tfrac12 g\,(Y/2K)^{\frac12}H\,(1 - 15H/16 + 35H^2/256\,..) \end{aligned} \qquad \text{(A2.5)}$$

For a three-halves-law amplifier $f(v) = (2/3)\,vf'(v)$. From this it can easily be shown that $G_0 - 5G_2 = 4\,(H-1)\,G_1$. Since $G_0 - G_2 = -1/R_K$, $-G_2 R_K = G_2/(G_0 - G_2)$ and, from the above, $-G_1 R_K =$

$(1 + 4G_2R_E)/4(H - 1)$. Hence $-G_1R_E$ and $-G_2R_E$ can be calculated as functions of H (Fig. 6).

Since $(V_e \cos x + V_g - V_{ca})^{\frac{1}{2}}$ is a positive decreasing function of x in the range $0 < x < \pi$, it follows that for the three-halves-law amplifier $G_1 > 0$. The inequality $G_1^2 - G_0G_2 > 0$ is also of some importance. Since $G_0 > 0$ the inequality is satisfied when $G_2 < 0$. Only values of $H < 1{\cdot}42$ need therefore be considered since it is only in this range that $G_2 > 0$ (Fig. 6). Using (A2.5) it is easily shown that the inequality is satisfied for all sufficiently small values of H, and the graphs of Fig. 6 can be used to show that it is also satisfied when $H > 0{\cdot}2$.

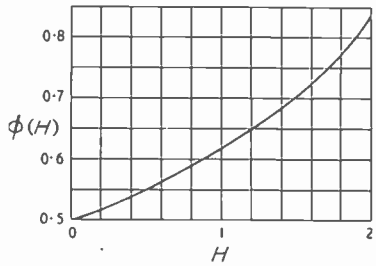

Fig. 17. *The function* $\phi(H)$.

APPENDIX 3

The Effect of Anode-Circuit D.C. Resistance on the Oscillation Amplitude

If I_a is the mean anode current and R_a the d.c. resistance, the mean anode voltage is less than the h.t. supply voltage by an amount I_aR_a. Let V'_{ca} be the grid voltage for anode-current cut-off when the mean anode voltage equals the supply voltage.

Then $V_{ca} - V'_{ca} = I_aR_a/\mu = (1 - n^2)\, V_{ca}$ .. (A3.1)

where $n^2 = V'_{ca}/V_{ca}$

Now $I_a = (1/\pi)\int_0^\pi f\,(V_e \cos x + V_g - V_{ca})\, dx + kV_g/R_g$

When $f\,(v)$ follows the three-halves law the integral can be expressed in terms of G_0 and G_1 by writing $f\,(v) = (2/3)\, vf'\,(v)$ and using (5.10).

Then $I_a = (2/3)\{V_eG_1 + (V_g - V_{ca})\, G_0\} + kV_g/R_g$

Substituting this into (A3.1) gives

$$n^2 - 1 = -\{\phi\,(H)/R_E + kK/R_g\}\, YR_a/\mu K \qquad \text{(A3.2)}$$

where $\phi\,(H) = -(2/3)\{G_0\,(H - 1) + G_1\}\, R_E$

This function is shown graphically in Fig. 17, using the values of G_0 and G_1 calculated in Appendix 2.

The oscillation amplitude can be found as follows. V'_{ca} is a known constant. Let $N' = -1\frac{1}{2}b_a\,(-V'_{ca})^{\frac{1}{2}}R_E$. Then $N = N'/n$. Assuming some plausible value for n, a value for Y can be read off from Fig. 3. This is used to find H and hence $\phi\,(H)$. A value for n can then be calculated from (A3.2). This will differ more or less from the assumed value. Using the new value of n, the calculation is repeated to find a third value, and the process is continued until no further improvement is obtained.

APPENDIX 4

The Effect of an Impedance in the Screen-Grid Circuit

In tetrodes and pentodes the grid–anode amplification factor is usually so large that, provided the valve operates above the 'knee' of the characteristic, the anode voltage has a negligible influence on anode current. If the screen-grid voltage varies the anode current can be expressed as $i_a = f\,(v_g + v_{as}/\mu_s - V_{ca}) - ki_g$, where v_{as} is the alternating screen voltage and μ_s is the grid–screen amplification factor. Usually the impedance in the screen circuit is a decoupling network having a negligible impedance at the oscillation frequency, so that in the steady state v_{as} is practically zero. Then $\theta = 0$ and $q = 1$.

The transient current is

$$i_{ad} = (v_{gd} + v_{sd}/\mu_s)\, f'\,(V_{g1} \cos \omega_0 t + V_g - V'_{ca}) - ki_{gd}$$

and $i_{ad} + ki_{gd} = (v_{gd} + v_{sd}/\mu_s) \sum_{-\infty}^{\infty} G_n \exp. jn\omega_0 t$ .. .. (A4.1)

where v_{sd} is the transient screen voltage. Since the screen and anode currents are in the ratio $(1 - k)/k$ it follows that $v_{sd} = -Z_s\,(D)\, i_{sd} = -Z_s\,(D)\, i_{ad}(1 - k)/k$, where $Z_s\,(D)$ is the screen circuit impedance. Substituting for i_{ad} from (6.1)

$$v_{gd} + v_{sd}/\mu_s = \{1 + Z_s\,(D)/\mu_1 Z_i\,(D)\}\, v_{gd} + \{Z_s\,(D)\, Z_0\,(D)/\mu_1 Z_i\,(D)\}\, i_{gd} \qquad \text{(A4.2)}$$

in which $\mu_1 = \mu_s k/(1 - k)$.

Now the corresponding quantity which is used in the equations of Sections 5 and 6 is

$v_{gd} + v_{ad}/\mu = \{1 + Z_i\,(D)/\mu Z_t\,(D)\}\, v_{gd} + Z_n\,(D)\, i_{gd}/\mu$.

Comparing this with (A4.2) and comparing (A4.1) with (5.9) it is seen that the equations of Sections 5 and 6 will be valid under the new conditions if μ is replaced by μ_1, $Z_i(D)$ by $Z_s(D)$, and $Z_n(D)$ by $Z_s(D)Z_0(D)/Z_t(D)$. Also Z_s^+ and Z_s^- will be negligible. Only Z_s^0 will have a significant value.

APPENDIX 5

Comparison with Previous Work

In a previous paper[19] amplitude-stability criteria for a symmetrical-circuit oscillator with $R_a = 0$ and having a three-halves-law amplifier were obtained. Although derived by very different methods these results are in agreement with those of the present paper when due allowance is made for the different approximations and symbols used.

Writing $Y = V_g/V_{ca}$ in (10.5), the criterion for aperiodic instability at large oscillation amplitudes becomes

$V_{ca}/V_g < (1 - K)/3K + (1 - K)^2/27K + \ldots$

or $V_g/V_{ca} > 3K/(1 - K) + \ldots$ which is the same as expression (8.9) of reference 19.

For symmetrical circuits $R_y = 0$. Putting also $R_a = 0$, $R_E = (R_T + R_I/\mu)/(1 - kR_T/r_g)$, $R_T = 1/G_t$, and $V_0 = 1/d$ in (10.8) gives the criterion for the existence of a hysteresis effect at the threshold of oscillation as

$$V_g/(V_g - V_{ca}) - \{R_0 + kr_g/(k - G_tr_g)\}(1 + dV_g)/(R_0 + r_g) > (1 - dV_g)\,(1 + G_tR_I/\mu)^2/4d^2\,(V_g - V_{ca})^2$$

This agrees with expression (8.7) of ref. 19 (note that in ref. 19 the symbol R_i has the same meaning as the R_I in the above formula. The values of the parameters are those at the inception of oscillation. In ref. 19 this is indicated by the accent ').

The criterion (11.8) for periodic stability can be rewritten as follows: Let $Q' = Qr_g/(R_0 + r_g)$; i.e., Q' is the Q-factor of the circuit when the extra damping due to grid current is included. Let $G_0 + G_2 = g_0'$, and let $1 + S_0R_g = S$. It will be sufficient to consider the case of $V_{cg} = 0$. Then Fig. 5 shows that over a wide range of b_gR_g, $S_2r_g = \frac{1}{2}S_0R_g$. Hence $S_2r_g = \frac{1}{2}\,(S - 1)$. Substituting these transformations into (11.8) and using also (4.11) and (5.14) the criterion for periodic instability becomes

$$2SQ'X_g/R_g < -r_g/(R_0 + r_g) - g_0'\,(R_I/\mu + 1/G_t) - S\,\{R_0/(R_0 + r_g) - k/G_tr_g\}$$

This agrees with expression (7.16) of ref. 19 when $V_{cg} = 0$. [Note that the symbol Q in (7.16) is equivalent to Q' in the above formula.]

It can also be shown that the auxiliary condition (7.15) in ref. 19 is always satisfied when (7.16) is satisfied. Hence the agreement is complete.

NEW FILTER THEORY OF PERIODIC STRUCTURES

By W. K. R. Lippert, Dr. rer. nat.

(Division of Building Research, Commonwealth Scientific and Industrial Research Organization, Melbourne, Australia)

(Concluded from p. 266, October issue)

7. Image Parameters and Characteristic Factors of Multi-Cascade-Connected Symmetrical Structures

The representation of the image parameters of equal cascade-connected filter sections is fairly simple, because one parameter, viz. the image impedance function Z_i, is not changed at all, as can be deduced from its definition. The attenuation function Q_n of n sections can be obtained from Q for one section by

$$\frac{Q_n + 1}{Q_n - 1} = \left(\frac{Q + 1}{Q - 1}\right)^n_{n = 2,3,4 \ldots} \qquad (33)$$

which is simple and well known[5]. In practice, however, cases frequently occur where it is not possible to control the frequency characteristic of Z_i and where the filter cannot be operated between terminating impedances which have approximately the same value as Z_i. In such cases an exact representation of the wave propagation with the image parameters requires corrections which can become rather complicated if n is small, so that the direct use of the characteristic factors is preferable.

It can be shown that the characteristic factors R_n and T_n of a four-terminal circuit which consists of n equal and symmetrical four-terminal circuits connected in cascade can also be derived in a general procedure from the characteristic factors R and T of one section. For the first four periodic structures this yields:

1 section:

$$R_1 \equiv R$$
$$T_1 \equiv T$$

2 sections:

$$R_2 = R\left[1 + \frac{T^2}{1 - R^2}\right]$$
$$T_2 = \frac{T^2}{1 - R^2}$$

3 sections:

$$R_3 = R\left[1 + \frac{T^2(1 - R^2 + T^2)}{(1 - R^2)^2 - R^2T^2}\right]$$
$$T_3 = \frac{T^3}{(1 - R^2)^2 - R^2T^2}$$

4 sections:

$$R_4 = R\left[1 + T^2\frac{(1 - R^2)^2 + T^2(1 - 2R^2 + T^2)}{(1 - R^2)^3 - R^2T^2(2 - 2R^2 + T^2)}\right]$$
$$T_4 = \frac{T^4}{(1 - R^2)^3 - R^2T^2(2 - 2R^2 + T^2)} \qquad (34)$$

A brief derivation of these equations is given in the Appendix. Equs. (34) are a standard set of general formulae for n-sectional periodic and symmetrical structures. Fortunately, these formulae can be greatly simplified in loss-free cases which are important in many practical applications. In these cases, a relation between R and T equivalent to Equ. (18) is valid:

$$R^2 = -(1 - B^2)\exp. j2\beta \qquad (35)$$

and this can be used to eliminate R in the values of T_n of Equs. (34). As $T = B\exp. j\beta$ [cf. Equ. (3)], the magnitudes B_n as well as the phase values β_n can be represented by B and β. This yields the following set of formulae for n-sectional periodic, loss-free and symmetrical structures:

1 section:

$$B_1 \equiv B$$
$$\beta_1 \equiv \beta$$

2 sections:

$$B_2 = \frac{B^2}{\sqrt{B^4 + 4(1 - B^2)\cos^2\beta}}$$
$$\beta_2 = \arctan\left[\frac{\sin 2\beta}{\cos 2\beta + 1 - B^2}\right] = \arctan\left[\frac{2\cos^2\beta}{2\cos^2\beta - B_2}\tan\beta\right]$$

3 sections:

$$B_3 = \frac{B^3}{\sqrt{B^4 - 8(1 - B^2)(B^2 - 2\cos^2\beta)\cos^2\beta}}$$
$$\beta_3 = \arctan\left[\frac{\sin 3\beta + (1 - B^2)\sin\beta}{\cos 3\beta + 3(1 - B^2)\cos\beta}\right] = \arctan\left[\frac{4\cos^2\beta - B^2}{4\cos^2\beta - 3B^2}\tan\beta\right]$$

4 sections:

$$B_4 = \frac{B^4}{\sqrt{B^8 + 16(1 - B^2)(B^2 - 2\cos^2\beta)^2\cos^2\beta}}$$
$$\beta_4 = \arctan\left[\frac{\sin 4\beta + 2(1 - B_2)\sin 2\beta}{\cos 4\beta + (1 - B^2)(4\cos 2\beta + 3 - B^2)}\right] = \arctan\left[\frac{8\cos^4\beta - 4B^2\cos^2\beta}{8\cos^4\beta - 8B^2\cos^2\beta + B^4}\tan\beta\right] \qquad (36)$$

This result is significant as Equs. (36) can be easily represented by diagrams if B is taken as the parameter, as has been shown elsewhere[3]. It is not necessary to use Equ. (34) to find R_n or A_n and α_n. These values can be derived immediately from B_n and β_n because Equ. (18) can be applied for loss-free n-sectional filters also:

$$A_n^2 + B_n^2 = 1$$

$$\alpha_n - \beta_n = \mp \frac{\pi}{2} \quad \ldots \quad \ldots \quad \ldots \quad (37)$$

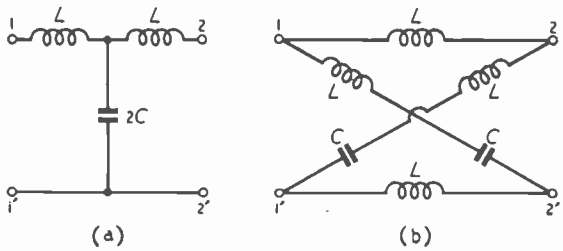

Fig. 6. *Example of a T-type low-pass filter (a), and equivalent lattice-type circuit (b).*

8. Examples

To illustrate the usefulness of the theory the characteristic factors of a simple so-called T-type low-pass filter of Fig. 6(a) will be derived and the frequency characteristics of some periodic structures with these filters will be described. The T-type filter of Fig. 6(a) can be transformed to the equivalent lattice type filter of Fig. 6(b) with the aid of Bartlett's theorem[6]. The impedances Z_1 and Z_2 of the two arms are:

$$Z_1 = j\omega L$$

$$Z_2 = j\omega L + 1/j\omega C \quad \ldots \quad \ldots \quad (38)$$

The (circular) cut-off frequency is

$$\omega_0 = 1/\sqrt{LC} \quad \ldots \quad \ldots \quad \ldots \quad (39)$$

For the purpose of finding the characteristic factors at first the value of the reference impedance Z_R has to be chosen. This can be done by relating it to a suitable circuit element. In this particular case Z_R may be specified by:

$$Z_R = \epsilon \sqrt{\frac{L}{C}} \quad \ldots \quad \ldots \quad \ldots \quad \ldots \quad (40)$$

where

L = inductance
C = capacitance
ω = circular frequency
ϵ = positive dimensionless factor (for selecting a particular value of Z_R)

The functions p and q are in this case given by the following relation:

$$p^2 = \frac{1}{\epsilon^2}\left(1 - \frac{\omega^2}{\omega_0^2}\right) \quad \ldots \quad \ldots \quad \ldots \quad (41)$$

and $q^2 = 1 - \dfrac{\omega_0^2}{\omega^2} \quad \ldots \quad \ldots \quad \ldots \quad \ldots \quad (42)$

and this yields with Equ. (29):

$$B^2 = \frac{1}{1 + \dfrac{1}{\epsilon^2}\dfrac{\omega^2}{\omega_0^2}\left(\dfrac{\omega^2}{\omega_0^2} + \epsilon^2 - 1\right)^2} \quad \ldots \quad (43)$$

and with Equ. (30)

$$\cos^2\beta = B^2\left(2\frac{\omega^2}{\omega_0^2} - 1\right)^2 \quad \ldots \quad \ldots \quad (44)$$

For this example, the values of B and β have been plotted against ω/ω_0 for various values of ϵ in Fig. 7(a) and (b). With the aid of such a set of curves for B and β, which are considered to be suitable co-ordinates in the sense of the theory developed above, the frequency characteristics of periodic structures as shown in Fig. 8 can be easily derived. A particular structure is determined by the value of ϵ, which can be found from Z_R [cf. Equ. (40)], by the length $l/2$ of the transmission line at the input and output of each section and by the number n of the sections. (The value of the reference impedance Z_R of the four-terminal circuit must, of course, be equal to that of the characteristic impedance of the transmission lines.) At first the curves of B and β which belong

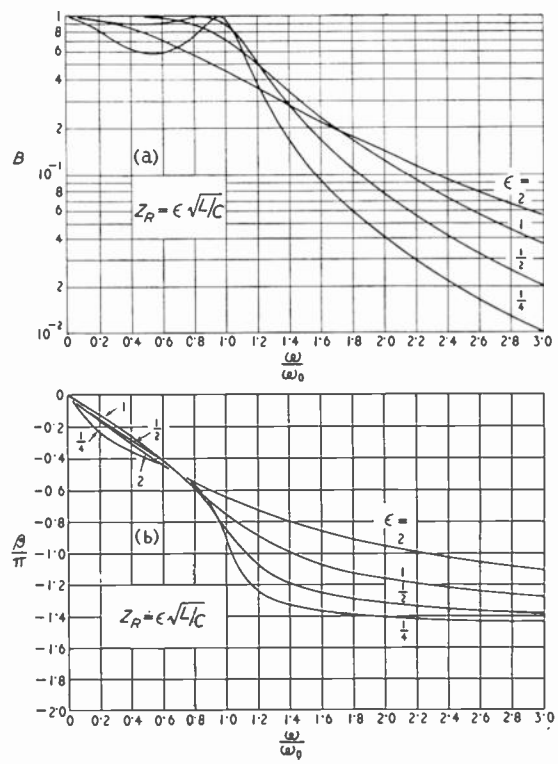

Fig. 7. *(a) Magnitudes B, and (b) phase values β/π of the characteristic transmission factors of the low-pass filter of Fig. 6 plotted against ω/ω_0 for various values of ϵ.*

to a particular value of ϵ can be taken from Fig. 7(a) and (b), then the values of β are transformed to β' which belong to one section consisting of the low-pass filter and the piece of transmission line connected at the input and output. This transformation is from Equ. (5):

$$\beta' = \beta - 2\pi \frac{l}{\lambda} = \beta - 2\pi \frac{l}{\lambda_0} \frac{\omega}{\omega_0} \quad \ldots \quad (45)$$

where λ_0 is the wavelength on the transmission line for $\omega = \omega_0$. For simplicity it has been assumed in Equ. (45) that λ is inversely proportional to ω or that the phase velocity does not depend on ω. (In more general cases, however, it has to be observed that the particular relation between λ and ω may be different.) The values of B and β' can then be used to determine B_n and β_n of the n-section filter with the aid of diagrams of Equ. (36) which are presented in the earlier paper[3]. This has been done in Fig. 9(a) and (b) where the frequency characteristics are plotted for the following examples:

for $\epsilon = \frac{1}{4}$ (or $Z_R = \frac{1}{4}\sqrt{L/C}$) and for $l = 0$ and $n = 1$ and 2 and for $l = \lambda_0/8$ and $n = 1$ and 2, and in Fig. 10(a) and (b) for $\epsilon = 2$ (or $Z_R = 2\sqrt{L/C}$) and for $l = 0$ and $n = 1$, for $l = \lambda_0/4$ and $n = 1$ and 2 and for $l = 3\lambda_0/8$ and $n = 1$ and 3. These examples show the workability of the theory and its ease of application. The resultant frequency characteristics of the periodic structures which are derived here in a systematic way are rather complex functions. The inconvenience of determining the characteristic factors for various values of ϵ is amply compensated by the simplicity of the transformation of Equ. (45) and the possibility of using the diagrams of Equs. (36).

In cases where the four-terminal circuits are not loss-free, the general Equs. (34) have to be used instead of diagrams and the work involved is usually greater. However, even in such cases the method presented here is applicable and for a particular example the derivation of the characteristic factors of a single filter section will be described.

Fig. 11 shows a T-type four-terminal circuit which consists of two series resistances (r) and a shunt capacitance ($2C$) and its equivalent lattice-type circuit[6]. The values of Z_1 and Z_2 are in this case:

$$Z_1 = r$$
$$Z_2 = r + 1/j\omega C \quad \ldots \quad \ldots \quad \ldots \quad (46)$$

with the following relations

$$\omega_0 = 1/rC \quad \ldots \quad \ldots \quad \ldots \quad \ldots \quad (47)$$

and

$$Z_R = \eta r \quad \ldots \quad \ldots \quad \ldots \quad \ldots \quad (48)$$

where η has a similar meaning to that of ϵ in the loss-free case of Equ. (40); the functions P and Q are from Equ. (25):

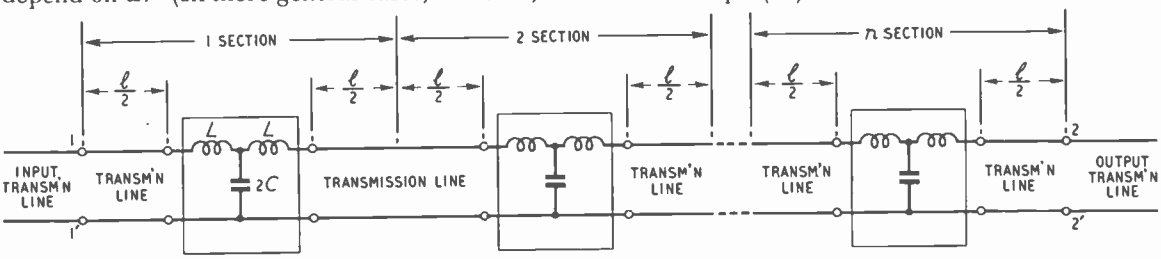

Fig. 8. *Example of a n-sectional periodic structure. (Low-pass filters of Fig. 6 with a length l/2 of a transmission line connected at the input and output of each section.)*

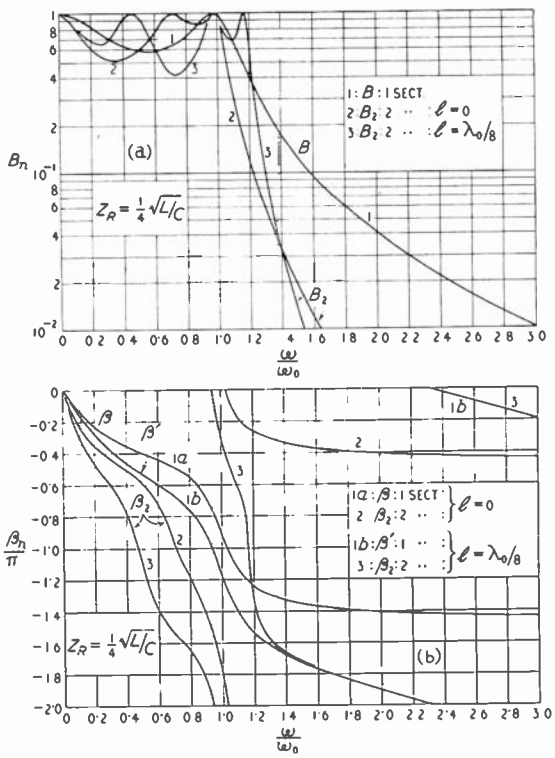

Fig. 9. *(a) Magnitudes B, B_2 and (b) phase values β/π, β'/π, β_2/π of the characteristic transmission factors of the periodic structures of Fig. 8 plotted against ω/ω_0 for $\epsilon = \frac{1}{4}$ (or $Z_R = \frac{1}{4}\sqrt{L/C}$), for $l = 0$ and $n = 1$ and 2 and for $l = \lambda_0/8$ and $n = 1$ and 2.*

$$P = \frac{1}{\eta}\sqrt{1 - j\frac{\omega_0}{\omega}}$$

and

$$Q = \sqrt{1 - j\frac{\omega_0}{\omega}} \qquad \ldots \quad \ldots \quad \ldots \quad (49)$$

These values yield with the aid of Equ. (26)

$$R = \frac{1}{1+\eta}\,\frac{1 + j(1-\eta^2)\,\omega/\omega_0}{1 + j(1+\eta)\,\omega/\omega_0}$$

and

$$T = \frac{\eta}{1+\eta}\,\frac{1}{1 + j(1+\eta)\,\omega/\omega_0} \qquad \ldots \quad (50)$$

Hence, the required magnitudes and phase values of the characteristic factors can be easily found

$$A = \frac{1}{1+\eta}\sqrt{\frac{1 + (1-\eta^2)^2\,\omega^2/\omega_0^2}{1 + (1+\eta)^2\,\omega^2/\omega_0^2}}$$

$$\alpha = -\arctan\left[\frac{\eta(1+\eta)\,\omega\,\omega_0}{1 + (1-\eta^2)\,(1+\eta)\,\omega^2/\omega_0^2}\right]$$

$$B = \frac{\eta}{1+\eta}\,\frac{1}{\sqrt{1 + (1+\eta)^2\,\omega^2/\omega_0^2}}$$

$$\beta = -\arctan\,(1+\eta)\,\omega/\omega_0 \qquad \ldots \quad (51)$$

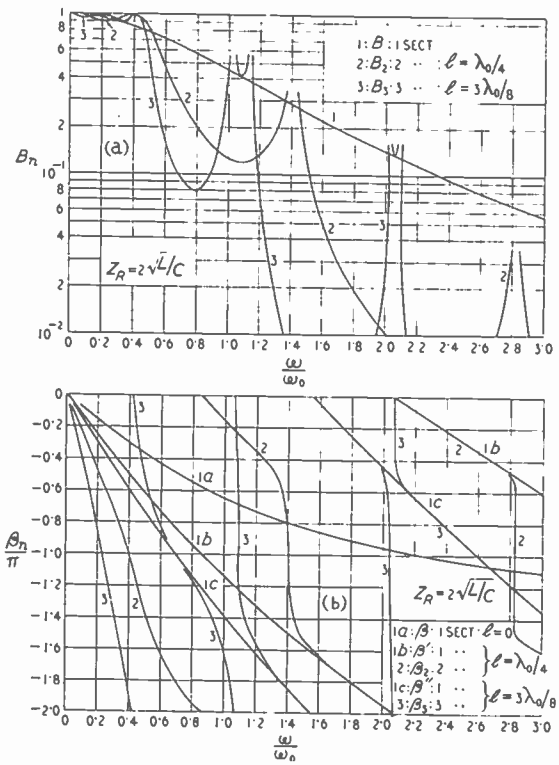

Fig. 10. *(a) Magnitudes B, B_2, B_3 and (b) phase values β/π, β'/π, β''/π, β_2/π, β_3/π of the characteristic transmission factors of the periodic structure of Fig. 8 plotted against ω/ω_0 for $\epsilon = 2$ (or $Z_R = 2\sqrt{L/C}$), for $l = 0$ and $n = 1$, for $l = \lambda_0/4$ and $n = 1$ and 2, and for $l = 3\lambda_0/8$ and $n = 1$ and 3.*

If a periodic structure similar to the loss-free one shown in Fig. 8 but with four-terminal circuits as in Fig. 11(a) has to be described, the four values A, α, B and β of Equ. (51) can be plotted against ω/ω_0 for various values of η and the values of α and β can be transformed with the aid of Equ. (5) in the same way as has been shown in Equ. (45) for the loss-free case.

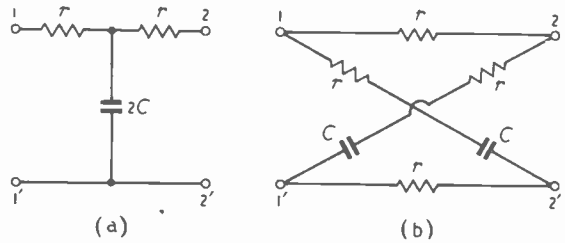

Fig. 11. *Example of a symmetrical four-terminal circuit with resistances (a), and its equivalent lattice-type circuit (b).*

9. Discussion

The characteristic reflection and transmission factors of a four-terminal circuit are, as has been shown above, a particular generalization of the conventional circuit constants. The reference impedance plays the part of a useful parameter for determining the appropriate characteristic factors in particular filter problems. The use of the characteristic factors can greatly simplify the theoretical work involved which shows that these factors are suitable circuit constants in the theory of periodic structures.

The characteristic transmission factor has a simple relation to the insertion ratio [cf. Equ. (11)] of a four-terminal circuit connected to two equal resistances R_0 at the input and output (cf. Fig. 2). Therefore, the frequency characteristics of T for various values of Z_R represent the usually required operating characteristics of a loss-free filter [cf. Fig. 7(a) and (b)]. In some practical cases it can happen that the value of $Z_R(= Z_0)$ is real, but varies with frequency. However, even in such cases the required frequency characteristic of T can be found by interpolation from a set of curves with constant values of Z_R as shown in the instance of Fig. 7(a) and (b).

The particular value of the characteristic factors is obviously their usefulness in the theory of periodic and symmetrical structures with not too many sections. Two features are significant: the simplicity with which these factors can be transformed in those frequent and practical cases where it is necessary to discuss the frequency characteristics if the length of the transmission lines connected at the input and output of one section is changed, and the general and straightforward procedure which can be used to derive the

characteristic factors of n sections. The major simplifications in loss-free cases, where most of the work can be done with the aid of diagrams, are also important.

If the characteristic factors R and T which belong to a symmetrical filter and a particular value of $Z_R (= R_0$; cf. Fig. 2) are known or have been measured, and the problem is to find the characteristic factors R' and T' which belong to another value Z'_R then this can be solved with the aid of Equs. (25) and (26). Q is not changed at all and for P' it yields:

$$P' = \frac{Z_R}{Z'_R} P = \frac{P}{\kappa} \qquad \ldots \quad \ldots \quad \ldots \qquad (52)$$

where κ is a dimensionless factor.

With Q and P' the values R' and T' can then be determined from Equ. (26).

$$R' = \frac{2R(1+\kappa^2) + (1+R^2-T^2)(1-\kappa^2)}{(1+\kappa)^2 + 2R(1-\kappa^2) + (R^2-T^2)(1-\kappa)^2}$$

$$T' = \frac{4\kappa T}{(1+\kappa)^2 + 2R(1-\kappa^2) + (R^2-T^2)(1-\kappa)^2}$$

$$Z'_R = \kappa Z_R \qquad \ldots \quad \ldots \quad \ldots \qquad (53)$$

This could have been derived in a similar way from Equ. (20) and its reversal. An extension of Equs. (53) to general asymmetrical cases is also possible with the aid of Equs. (14) and (15). It may be observed, however, that such a transformation of the characteristic factors for various values of Z_R (or κ) is only valid if a change of Z_R does not change the particular wave form (mode of wave) at the terminals. In certain analogies to an electrical transmission line (e.g., in waveguide systems or acoustical ducts) it is well known that in some frequency ranges different modes of waves are possible. In such cases, any analogy to electrical transmission lines is restricted to only one mode which can be propagated practically without attenuation and to a frequency range where the other modes are attenuated or not excited. These other modes will usually occur within the four-terminal circuits of a periodic structure to fulfil certain boundary conditions but they should not be present at the various terminals or at the equivalent reference planes.

Another practical problem is to show how the reflection and transmission factors are modified if the load resistance at the output alone is changed or if a periodic filter is terminated by a non-equal section or by a reflecting line. This has been investigated and the results are quoted briefly for symmetrical four-terminal circuits in the earlier paper[3] and will be omitted here.

Finally, it may be observed that the method investigated above is restricted to real values of the characteristic impedance of the transmission lines (reference impedance). The method may occasionally be applicable also in cases where the value of the reference impedance is complex; e.g., if the losses on a transmission line are small and can be represented approximately by a (lumped) resistance which is included in the four-terminal network (cf. Fig. 11); but in general complex values of the reference impedance require another investigation.

The four-terminal networks applied in the various periodic structures have not necessarily to be constructed by lumped circuit elements alone. They can consist of any system that is equivalent to a four-terminal network in the sense that the fundamental relations [Equ. (12)] for linear and passive systems are applicable. The method has been used and checked by the author recently in experimental work on the sound propagation in acoustical ducts with bends[7]. Therefore (and according to what has been said above and in the introduction) the concept of the characteristic factors may well prove useful in defining the transmission functions in analogous electrical work too; e.g., in waveguide or other ultra-high-frequency techniques.

10. Conclusions

1. The 'characteristic reflection and transmission factors' form a set of functions in terms of which a theory of four-terminal networks (e.g., filters) can be derived.

2. The 'characteristic reflection and transmission factors' can be specified quantitatively in various ways; e.g., in terms of certain characteristics of the standing-wave pattern on lines connected to the input and output of the network under discussion, in terms of certain characteristics if the network has known constant impedance terminations or in terms of certain relationships with the usual circuit constants.

3. The 'characteristic factors' can be used profitably for describing the reflection and transmission of waves in the filter theory of specific periodic and symmetrical structures.

4. The use of the 'characteristic factors' leads to major simplifications in the theory of loss-free structures where most of the work can be done with the aid of diagrams.

Acknowledgment

The author wishes to thank Mr. A. E. Ferguson of the Electrical Engineering Department of the University of Melbourne for kindly reading the manuscript and for constructive criticism of the presentation of the argument.

APPENDIX

Equ. (34) can be derived in the following way[3]: For a symmetrical network $Z_{11} = Z_{22}$ and Equs. (12) become:

$$E_1 = Z_{11} I_1 + Z_{12} I_2$$
$$E_2 = Z_{12} I_1 + Z_{11} I_2 \qquad \ldots \quad \ldots \quad \ldots \qquad (54)$$

The coefficients of the impedance matrix are related to the characteristic reflection and transmission factors R and T and the reference impedance Z_R by [cf. Equ. (15)]

$$\frac{Z_{11}}{Z_R} = \frac{1 - R^2 + T^2}{(1 - R)^2 - T^2}$$

$$\frac{Z_{12}}{Z_R} = \frac{2T}{(1 - R)^2 - T^2} \qquad \ldots \quad \ldots \quad \ldots \quad (55)$$

Equ. (54) can be transformed to the following form

$$\begin{aligned} E_1 &= aE_2 - bI_2 \\ I_1 &= cE_2 - aI_2 \end{aligned} \qquad \ldots \quad \ldots \quad \ldots \quad (56)$$

and this yields the 'general circuit' constants a, b, c, [where the negative sign in Equ. (56) is caused by the choice of the direction of I_2 in Figs. 1(a) and 2].

With the aid of Equs. (54) to (56) the general circuit constants can be represented by the characteristic factors:

$$a = \frac{1 - R^2 + T^2}{2T}$$

$$b = \frac{(1 + R)^2 - T^2}{2T} \cdot Z_R$$

$$c = \frac{(1 - R)^2 - T^2}{2T} \cdot \frac{1}{Z_R} \qquad \ldots \quad \ldots \quad \ldots \quad (57)$$

where the following relation is fulfilled

$$a^2 - bc = 1 \qquad \ldots \quad \ldots \quad \ldots \quad (58)$$

This yields the characteristic factors in terms of the general circuit constants:

$$R = \frac{b/Z_R - cZ_R}{2a + b/Z_R + cZ_R}$$

$$T = \frac{2}{2a + b/Z_R + cZ_R} \qquad \ldots \quad \ldots \quad \ldots \quad (59)$$

If n equal symmetrical filters (with the general circuit constants, a, b, c, a) are connected in cascade the general circuit constants of the resultant filter may be called a_n, b_n, c_n, a_n and they can be obtained by simple matrix algebra:

$$\left\| \begin{matrix} a_n & b_n \\ c_n & a_n \end{matrix} \right\| = \left(\left\| \begin{matrix} a & b \\ c & a \end{matrix} \right\| \right)^n \qquad \ldots \quad \ldots \quad \ldots \quad (60)$$

Equ. (60) is equivalent to:

$$a_n = aa_{n-1} + \sqrt{(a_{n-1}^2 - 1)(a^2 - 1)}$$

$$\frac{b_n}{b} = \frac{c_n}{c} = \sqrt{\frac{a_n^2 - 1}{a^2 - 1}} \qquad \ldots \quad \ldots \quad \ldots \quad (61)$$

As $a_1 \equiv a$, this yields

$$\begin{aligned} a_2 &= 2a^2 - 1 \\ a_3 &= 4a^3 - 3a \\ a_4 &= 8a^4 - 8a^2 + 1 \\ &\ldots \end{aligned} \qquad \ldots \quad \ldots \quad \ldots \quad (62)$$

and

$$\frac{b_2}{b} = \frac{c_2}{c} = 2a$$

$$\frac{b_3}{b} = \frac{c_3}{c} = 4a^2 - 1$$

$$\frac{b_4}{b} = \frac{c_4}{c} = 8a^3 - 4a \qquad \ldots \quad \ldots \quad \ldots \quad (63)$$

$$\ldots$$

[It may be observed that it so happens that the polynomials of Equs. (62) and (63) are obviously identical with the so-called Tschebyscheff's polynomials $T_n(a)$ and $Q_{n-1}(a)$ which are specified in textbooks[8].] If n equal and symmetrical filter sections are connected in cascade the resultant network is still a symmetrical filter and therefore the coefficients a_n, b_n, c_n, a_n are related to the characteristic factors $R_n = A_n \exp. j\alpha_n$ and $T_n = B_n \exp. j\beta_n$ by a formula identical in form to equations (59), viz.

$$R_n = \frac{b_n/Z_R - c_nZ_R}{2a_n + b_n/Z_R + c_nZ_R}$$

$$T_n = \frac{2}{2a_n + b_n/Z_R + c_nZ_R} \qquad \ldots \quad \ldots \quad \ldots \quad (64)$$

With the aid of this formula and Equs. (61) [or Equs. (62) and (63)] and Equs. (57) the required relation between R_n, T_n and R, T as given in Equs. (34) can be determined.

REFERENCES

[1] L. Brillouin, "Wave Propagation in Periodic Structures", McGraw-Hill, New York, 1946.

[2] W. P. Mason, "Electromechanical Transducers and Wave Filters", D. Van Nostrand Comp., Inc., New York, 1946.

[3] W. K. R. Lippert, "A New Method of Computing Acoustical Filters", *Acustica*, 1954, Vol. 4, p. 411.

[4] W. K. R. Lippert, "A Method of Measuring Discontinuity Effects in Ducts", *Acustica*, 1954, Vol. 4, p. 307.

[5] W. Cauer, "Theorie der Linearen Wechselstromschaltungen" Akad. Verlagsges., Leipzig, 1941.

[6] A. C. Bartlett, "An Extension of a Property of Artificial Lines", *Phil. Mag.*, 1927, Vol. 7, p. 902.

[7] W. K. R. Lippert, "The Measurement of Sound Reflection and Transmission at Right-angled Bends in Rectangular Tubes", *Acustica*, 1954, Vol. 4, p. 313.

[8] E. Madelung, "Die mathematischen Hilfsmittel des Physikers", Springer-Verlag, Berlin-Göttingen-Heidelberg, 1950.

MEETINGS

I.E.E.

9th November. "A Transistor Digital Fast Multiplier with Magneto-Strictive Storage", by G. B. B. Chaplin, Ph.D., R. E. Hayes, B.Sc. and A. R. Owens, B.Sc.

14th November. "Is the Engineer Broad Enough in his Outlook?", discussion to be opened by P. Dunsheath, C.B.E., M.A., D.Sc.(Eng.).

15th November. "An Electrolytic-Tank Equipment for the Determination of Electron Trajectories, Potential and Gradient", and "A Method of Tracing Electron Trajectories in Crossed Electric and Magnetic Fields", by J. H. Westcott, Ph.D., B.Sc.

21st November. "The Reception of Band I and Band III Television Programmes", discussion to be opened by E. P. Wethey, B.Sc.

29th November. "The Specification of the Properties of the Thermistor as a Circuit Element in Very-Low-Frequency Systems" and "A Vector Method for Amplitude-Modulated Signals", by C. J. N. Candy, Ph.D., B.Sc.(Eng.).

1st December. "TRIDAC—A Large Analogue Computing Machine", by Lt.-Cdr. F. D. R. Spearman, J. J. Gait, M.A., B.Sc., A. V. Hemingway, B.Sc.(Eng.) and R. W. Hynes, B.Sc.

These meetings will be held at the Institution of Electrical Engineers, Savoy Place, Victoria Embankment, London, W.C.2 and will commence at 5.30.

Brit. I.R.E.

30th November. "High Fidelity Loudspeakers: The Performance of Moving-Coil and Electrostatic Transducers", by H. J. Leak, to be held at 6.30 at the London School of Hygiene and Tropical Medicine, Keppel Street, Gower Street, London, W.C.1.

The Television Society

11th November. "The Application of Semi-Conductor Diodes to Television Circuits", by J. I. Missen, M.Sc.

24th November. "Interference with Television Reception: Its Causes and Cures", by R. A. Dilworth.

These meetings will be held at 7 o'clock at the Cinematograph Exhibitors' Association, 164 Shaftesbury Avenue, London, W.C.2.

NEW BOOKS

Electrical Measurements and Measuring Instruments. (4th Edition)

By E. W. Golding, M.Sc.Tech., M.I.E.E., Mem. A.I.E.E. Pp. 913 + xiii. Sir Isaac Pitman & Sons Ltd., Parker Street, Kingsway, London, W.C.2. Price 40s.

A really fundamental approach to underlying physical theory, a detailed discussion of instruments and their applications in terms intelligible to degree students, and copious references to original papers—in all these respects the fourth edition of Mr. Golding's excellent book maintains the standard which has made it so valuable as a textbook and a work of reference. The proliferations of modern technique have been skilfully digested into the main body of the book, without discarding older methods which are educationally useful, so that the reader is given a picture of the growth and development of electrical measurements up to the present time.

Faced with the problem of revising a standard work at a time when ideas on the teaching of electricity are somewhat fluid, the author has decided to preserve the absolute c.g.s. treatment of the introductory theory. One cannot quarrel with this decision, for continuity with previous editions is a consideration and in any case the main interest of the book is in the practical side. Yet the urge to adopt the rationalized m.k.s. system came in the first place from those who believed in its advantages to the electrical engineer, and one has begun to expect these advantages to be demonstrated. There is, of course, a full and rather impartial discussion of units and dimensions in which the traditional outlook is fully represented.

While the book as a whole has been brought comprehensively up to date, the chief additions are in Chapter VII on resistance strain gauges, in Chapter XVII on amplifier-driven and servo-operated meters, and the new Chapter XXIII on thermionic devices, including the theory of negative feedback and velocity feedback, pulse-rate counters and Q-meters. The distribution of electronic accessories throughout the book would have justified an earlier place for the treatment of elementary thermionic valve theory.

It should be emphasized that the main purpose of the book is to explain the basic physical principles of electrical measurements to the student. In doing this, it does exemplify extremely well the kind of positive feedback that must be provided by the experienced electrical engineers of this generation to energize the specialists of the future. G.R.N.

Die physikalischen Grundlagen der Hochfrequenztechnik

By H. G. Möller. Pp. 261 + xiv with 288 illustrations. Springer-Verlag, Reichpietschufer 20, Berlin, W.35. Price DM 29.40.

The third edition of this book has been completely rewritten, and it now forms the first of five volumes on radio telegraphy being issued by von Korshenewsky of Stockholm and W. T. Runge of Berlin. The author of this volume is a Professor at Hamburg University. Of the other four volumes only one has been published, the other three are being prepared. This first volume is an introduction to the other volumes and lays the physical and mathematical foundation for all the special problems considered in them.

The first chapter deals with oscillatory circuits, resonance, measurements and calculations of inductance, capacitance, loss and damping due to the eddy currents, hysteresis, etc., bandwidth, selectivity and Q, band-filters and discriminators. One must not be misled by the title of the book: the treatment is mathematical and assumes a fairly wide physical knowledge of the subject.

The second chapter deals with valves, their fundamental principles and their various applications; the treatment is very thorough and occupies about seventy pages, much of it very mathematical.

The third chapter deals with the transmission and radiation of waves along Lecher wires and waveguides and in space, including the ionosphere. The fourth chapter is entitled "decimetre and centimetre wave technique", and deals with klystrons, magnetrons, and travelling-wave tubes. The fifth chapter of three and a half pages describes impulse testing methods using cathode-ray tubes, as employed in radar and allied devices. In the sixth chapter shot effect and noise in valves and resistances are discussed and their calculation and measurement, while in the final chapter the fundamental physical properties of rectifiers and transistors are treated. In a footnote it is stated that this subject is dealt with more fully by Strutt in Vol. III, but, unless the notice at the end of the book is in error, this should be Vol. IV.

The book has two appendices, one of 28 pages, devoted to a more detailed explanation of the mathematics involved, such as complex quantities, Laplace transforms, four-poles, matrices, and vector algebra. The other appendix of 16 pages discusses fundamental laws of electricity and magnetism, such as those of Coulomb, Maxwell, and Poynting. There is an index, but one which only gives references to the pages of the book and not to original publications; this is a lack in such a book, but occasional references are given in the text and in footnotes. One is surprised to find in the index Plank for Planck, Jankè for Jahnke, and Goubeau for Goubau—all well-known names in German science; the last mistake occurs several times in the text.

In the formula $\mathcal{E} = 120\pi\,\Omega\,\frac{Ih_{eff}}{\lambda r}$ given on p. 1 for the field strength due to an aerial, the symbol Ω has crept in, apparently in the course of substitution from another equation, to which it is attached as an abbreviation for ohms, although in the index it is stated to be the symbol for tone frequency or solid angle.

The book contains a great amount of information on practically every branch of the subject, but is in no sense an elementary textbook, since it assumes from the very beginning a fairly high standard in both physics and mathematics. This is unavoidable when such a wide field has to be covered. A large number of numerical examples are given throughout the book. G.W.O.H.

***Wireless World* Diary 1956**

Pp. 79 of reference material and pp. 2 per week diary. Size 4½ in. by 3⅛ in. Iliffe & Sons Ltd., Dorset House, Stamford Street, London, S.E.1. Price 4s. 1d. (rexine), 5s. 10d. (leather), postage 2d. extra.

BRITISH STANDARDS

Components and Filter Units for Radio Interference Suppression

Pp. 37. B.S. 613:1955. Price 6s.

General Aspects of Radio Interference Suppression

Pp. 60. C.P.1006:1955. Price 10s.

These two publications are complementary. B.S. 613 is a second revision of one first published in 1935 and

revised in 1940. It covers the characteristics, ratings and markings of inductors, capacitors and resistors to be used for interference suppression.

The Code of Practice C.P.1006, deals with the use of such components to suppress interference generated by electric motors, thermostats, neon signs and so on. It is concerned mainly with the principle of suppression and explains the ways in which interference can reach a receiver. The effect of aerial siting is briefly considered and the booklet contains a number of photographs illustrating the appearance of different kinds of interference on a television picture.

The discussion is confined to interference on frequencies below 68 Mc/s. It does not cover Bands II or III.

British Standards Institution, 2 Park Street, London, W.1.

NEW DEFINITION OF THE UNIT OF TIME AND FREQUENCY

By L. Essen

(Communication from the National Physical Laboratory)

At the IXth General Assembly of the International Astronomical Union in Dublin, 29th August – 5th September 1955, several resolutions having a bearing on the measurement of frequency were adopted[1]. They will affect only the most precise measurements and the effect will not be immediate; but they are nevertheless of considerable importance and interest.

For the first time a rigid definition of the unit of time "the second" has been given. It is 1/31556925·975 of the tropical year for 1900. This unit has the great advantage of being invariable, unlike the mean solar second which is subject to annual and other variations; but it has the disadvantage of being less accessible; and for this reason a statement was appended to the definition outlining the present procedure to be adopted and giving the relationship between Universal Time and the new Ephemeris Time and between the frequencies as expressed in the two units.

Ephemeris time is determined in practice from observations of the position of the moon relative to the stars and it is estimated that in order to obtain an accuracy of 1 part in 10^9 which is now required for some purposes the observations will need to be extended over a period of about 4 years. The physicist or radio engineer is therefore left with the problem of dividing into equal seconds this long interval of time, and also of extrapolating beyond the astronomical observations so that the unit will be immediately available.

Quartz clocks have in the past served these purposes in the determination of Universal Time; but in this case the stellar observations are far more accurate than the moon observations and the interpolation was needed over correspondingly shorter periods. It is very doubtful whether quartz clocks preserve a sufficiently uniform rate to enable the ephemeris second to be determined with a precision of 1 part in 10^9; but fortunately the recent developments with atomic standards[2] suggest that these can be used to control the frequency of the quartz clocks to that degree of accuracy. Controlled in this way the quartz clocks will be adequate for their new and important function, but until the atomic frequency has been determined precisely in terms of the ephemeris second the clocks cannot be used for extrapolation purposes.

Universal Time will therefore still be used for civil purposes, but the annual variation and a variation due to the movement of the earth's pole will be smoothed out as far as possible, the same smoothing correction being used by all time services. The correction has not been easy to determine in the past but the increasing use of the photographic zenith tube for the astronomical measurements together with the use of the atomic standards should bring about a considerable improvement, and enable the variations in Universal Time to be smoothed out more completely in the future.

A provisional uniform time of this nature has been used in the determination of the value of the frequencies of the MSF standard transmissions since they were started in 1950 and the results have been published[3] in *Wireless Engineer* since 1952. The general adoption of Uniform Time will not therefore affect the method of determining the value of the MSF frequencies.

The N.P.L. quartz standard will, however, also be measured in terms of the atomic standard whenever the experimental programme permits this to be done, and the MSF transmissions will be measured in terms of the quartz standard. It will therefore be possible at a later date to express the frequencies of the transmissions from June 1955 in terms of the atomic standard and of the ephemeris second.

[1] Sir H. Spencer Jones, *Nature*, 1955, Vol. 176, p. 669.
[2] L. Essen and J. V. L. Parry, *Nature*, 1955, Vol. 176, p. 280.
[3] *Wireless Engineer*, March 1952.

STANDARD-FREQUENCY TRANSMISSIONS

(Communication from the National Physical Laboratory)

Values for September 1955

Date 1955 September	Frequency deviation from nominal: parts in 10^8	
	MSF 60 kc/s 1429-1530 G.M.T.	Droitwich 200 kc/s 1030 G.M.T.
1	+0·6	+1
2	+0·5	N.M.
3	N.M.	N.M.
4	N.M.	0
5	+0·5	0
6	+0·5	+3
7	+0·5	+3
8	+0·5	0
9	+0·5	0
10	+0·5	0
11	+0·5	0
12	+0·6	0
13	+0·6	0
14	+0·6	+1
15	+0·6	+1
16	+0·6	+1
17	+0·6	0
18	+0·6	0
19	+0·8	0
20	+0·8	+2
21	+0·6	+1
22	N.M.	+3
23	+0·6	−7
24	N.M.	0
25	N.M.	0
26	+0·8	+2
27	+0·7	+1
28	+0·8	+1
29	N.M.	+1
30	+0·7	+4

The values are based on astronomical data available on 1st October 1955.

N.M. = Not Measured.